



UNIVERSITY OF LEEDS

This is a repository copy of *Regional climate and vegetation response to orbital forcing within the mid-Pliocene Warm Period: A study using HadCM3*.

White Rose Research Online URL for this paper:
<http://eprints.whiterose.ac.uk/125410/>

Version: Accepted Version

Article:

Prescott, CL, Dolan, AM orcid.org/0000-0002-9585-9648, Haywood, AM orcid.org/0000-0001-7008-0534 et al. (2 more authors) (2018) Regional climate and vegetation response to orbital forcing within the mid-Pliocene Warm Period: A study using HadCM3. *Global and Planetary Change*, 161. pp. 231-243. ISSN 0921-8181

<https://doi.org/10.1016/j.gloplacha.2017.12.015>

(c) 2017, Elsevier B.V. This manuscript version is made available under the CC BY-NC-ND 4.0 license <https://creativecommons.org/licenses/by-nc-nd/4.0/>

Reuse

This article is distributed under the terms of the Creative Commons Attribution-NonCommercial-NoDerivs (CC BY-NC-ND) licence. This licence only allows you to download this work and share it with others as long as you credit the authors, but you can't change the article in any way or use it commercially. More information and the full terms of the licence here: <https://creativecommons.org/licenses/>

Takedown

If you consider content in White Rose Research Online to be in breach of UK law, please notify us by emailing eprints@whiterose.ac.uk including the URL of the record and the reason for the withdrawal request.

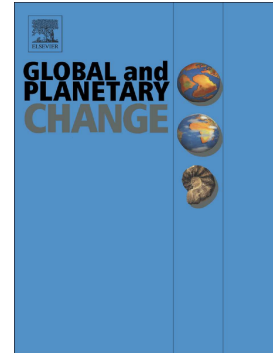


eprints@whiterose.ac.uk
<https://eprints.whiterose.ac.uk/>

Accepted Manuscript

Regional climate and vegetation response to orbital forcing within the mid-Pliocene Warm Period: A study using HadCM3

C.L. Prescott, A.M. Dolan, A.M. Haywood, S.J. Hunter, J.C. Tindall



PII: S0921-8181(17)30257-6
DOI: <https://doi.org/10.1016/j.gloplacha.2017.12.015>
Reference: GLOBAL 2699
To appear in: *Global and Planetary Change*
Received date: 19 May 2017
Revised date: 6 December 2017
Accepted date: 10 December 2017

Please cite this article as: C.L. Prescott, A.M. Dolan, A.M. Haywood, S.J. Hunter, J.C. Tindall, Regional climate and vegetation response to orbital forcing within the mid-Pliocene Warm Period: A study using HadCM3. The address for the corresponding author was captured as affiliation for all authors. Please check if appropriate. Global(2017), <https://doi.org/10.1016/j.gloplacha.2017.12.015>

This is a PDF file of an unedited manuscript that has been accepted for publication. As a service to our customers we are providing this early version of the manuscript. The manuscript will undergo copyediting, typesetting, and review of the resulting proof before it is published in its final form. Please note that during the production process errors may be discovered which could affect the content, and all legal disclaimers that apply to the journal pertain.

Regional climate and vegetation response to orbital forcing within the mid-Pliocene Warm Period: a study using HadCM3

^{1*}Prescott, C.L., ¹Dolan, A.M., ¹Haywood, A.M., ¹Hunter, S.J. and ¹Tindall, J.C

¹*School of Earth and Environment, University of Leeds, Woodhouse Lane, Leeds, LS2 9JT, UK.*

Corresponding author: C.L.Prescott (js07c2lp@leeds.ac.uk)

Abstract

Regional climate and environmental variability in response to orbital forcing during interglacial events within the mid-Piacenzian (Pliocene) Warm Period (mPWP; 3.264-3.025 Ma) has been rarely studied using climate and vegetation models. Here we use climate and vegetation model simulations to predict changes in regional vegetation patterns in response to orbital forcing for four different interglacial events within the mPWP (Marine Isotope Stages (MIS) G17, K1, KM3 and KM5c). The efficacy of model-predicted changes in regional vegetation are assessed by reference to selected high temporal resolution palaeobotanical studies that are theoretically capable of discerning vegetation patterns for the selected interglacial stages.

Annual mean surface air temperatures for the studied interglacials are between 0.4°C to 0.7°C higher than a comparable Pliocene experiment using modern orbital parameters. Increased spring/summer and reduced autumn/winter insolation in the Northern Hemisphere during MIS G17, K1 and KM3 enhances seasonality in surface air temperature. The two most robust and notable regional responses to this in vegetation cover occur in North America and continental Eurasia, where forests are replaced by more open-types of vegetation (grasslands and shrubland). In these regions our model results appear to be inconsistent with local palaeobotanical data. The orbitally driven changes in seasonal temperature and precipitation lead to a ~30% annual reduction in available deep soil moisture (2.0 m from surface), a critical parameter for forest growth, and subsequent reduction in the geographical coverage of forest-type vegetation; a phenomenon not seen in comparable simulations of Pliocene climate and vegetation run with a modern orbital configuration. Our results demonstrate the importance of examining model performance

under a range of realistic orbital forcing scenarios within any defined time interval (e.g. mPWP). Additional orbitally resolved records of regional vegetation are needed to further examine the validity of model-predicted regional climate and vegetation responses in greater detail.

1. Introduction

The mid-Piacenzian (Pliocene) Warm Period (mPWP), approximately 3.264 to 3.025 million years ago, was the most recent interval in Earth history when global annual mean temperatures are considered to have been higher than the pre-industrial (Haywood et al., 2013a; Dowsett et al., 2012). Atmospheric CO₂ concentration is estimated to range between 365 and 420 ppm through the mPWP (Pagani et al., 2010; Seki et al., 2010). A continually updated and large palaeoenvironmental reconstruction produced by the Pliocene Research Investigations and Synoptic Mapping (PRISM) project (e.g. Dowsett et al. 1994), in combination with numerous additional proxy data studies and modelling investigations, has enabled the mPWP to become a well-studied warm interval in Earth history (Haywood et al., 2013b). Primarily, the PRISM palaeoenvironmental reconstruction focussed on sea surface temperatures (SST), originally just for the North Atlantic (Dowsett & Poore, 1991) before further developing into a global reconstruction including vegetation cover. Applying a time slab approach (Dowsett & Poore 1991), the PRISM project reconstructed average interglacial conditions throughout the mPWP and found warming concentrated in the high latitudes, with minimal change in the tropics (Dowsett & Poore, 1991; Dowsett et al., 1994, 1996).

The PRISM vegetation reconstruction indicates a warmer and moister climate than today (Salzmann et al., 2008), with the largest differences found in the high latitudes related to a pronounced warming in this region (Thompson & Fleming, 1996). The warmer and wetter climate, on average, during the mPWP resulted in a northward shift of the taiga-tundra boundary and a spread of tropical savannahs and woodland in Africa and Australia at the expense of arid deserts (Salzmann et al., 2008).

To generate a satisfactory distribution of global vegetation data, the PRISM3 vegetation reconstruction incorporated records from the whole Piacenzian Stage of the Pliocene (~1 million years in duration; Salzmann et al. 2008). Most records within the reconstruction are

not dated on orbital timescales and could potentially represent interglacial or glacial conditions. However, where it was possible to reconstruct more than one potential biome from an individual locality, the biome representing the warmest climate condition was chosen (Salzmann et al. 2008).

While the PRISM3 vegetation synthesis is representative of the entire Piacenzian Stage, published vegetation records are available that can provide an indication of terrestrial climate variability in response to orbital forcing. For example, the joint pollen and marine faunal study in Japan by Heusser and Morley (1996), found temperatures varying between dry and humid conditions on top of an overall drying and cooling trend. Wu et al. (2011) found a general drying trend over the interior of central Asia reconstructed from sporopollen records. The Willis et al. (1999) sequence from Pula Maar (Hungary) showed significant fluctuations in vegetation between boreal and temperate forest, as well as dust data, thought to directly reflect changes in continental aridity and vegetation. Leroy and Dupont (1994) identified cyclic fluctuations between dry and humid periods in sediments dated 3.7 to 1.7 Ma in North West Africa and attributed these to marine isotope stages. The vegetation record from the James Bay Lowland in Canada shows fluctuations between deciduous and boreal forests in tune with the benthic oxygen isotope record (Gao et al., 2012). Tarasov et al. (2013) derived biome reconstructions based on pollen results from Lake El'gygytgyn in north-east Russia and found millennial-scale vegetation changes in the region that corresponded well with alternating cool and warm marine isotope stages during the mPWP. Finally, the record from Lake Baikal in south-central Siberia found short term intervals of climate deterioration controlling forest development and advances in open vegetation that overlay long term trends of cooling during the Pliocene (Demske et al., 2002). Here we investigate interglacial climate variability within, and immediately surrounding, the mPWP through examining four negative benthic oxygen isotope excursions. These are MIS G17, K1, KM3 and KM5c (Fig. 1) as seen in the LR04 benthic oxygen isotope stack (Lisiecki & Raymo, 2005). While it is important to look at cooler periods throughout the Pliocene to assess a complete picture of climate variability, the emphasis of this study is on the vegetation and climate response to orbital forcing during interglacial events. Concentrating on these warmer periods within the Pliocene is a natural progression from the original aims of the PRISM project to understand a past interval of global warmth (Dowsett

et al., 1999). This also enables the use of the PRISM3 datasets for boundary conditions for the climate model used here, which represent the warm phase of climate in the mPWP. These ‘super-interglacial’ events (Raymo et al., 2009) have also been targeted by the PLIOMAX (Pliocene Maximum Sea Level) project in a multidisciplinary approach to investigate Pliocene sea level high stands.

In this study, we analyse and compare the effect of orbital forcing on terrestrial climate and vegetation during these four interglacial events within the mPWP. We use a climate model with and without a dynamic vegetation component to answer the following questions:

1. How important is the effect of orbitally-driven seasonality changes for regional climate and land cover response during the interglacials studied, and how does the addition of a dynamic vegetation model alter the climatological as well as land cover response?
2. Looking at specific high resolution records (Lake Baikal and Lake El’gygytgyn), do our simulations capture similar variability shown in the geological record?

2. Methods

2.1 Model description

The Hadley Centre Coupled Climate Model Version 3 (HadCM3) is combined with either a dynamic vegetation model (Top-down Representation of Interactive Foliage and Flora Including Dynamics (TRIFFID)) or with a prescribed vegetation scheme. Two versions of the Met Office Surface Exchange Scheme (MOSES) are used; simulations with the dynamic vegetation model use the MOSES2.1 land surface scheme, and those with prescribed vegetation use MOSES1 to remain consistent with previous studies (e.g. Bragg et al., 2012; Prescott et al. 2014). We use the resulting modelled climatology to drive the BIOME4 model, which is an offline coupled biogeography and biogeochemistry model that simulates natural vegetation types (biomes). This allows a comparison of predicted biomes for all simulations directly to the Salzmann et al (2008) vegetation reconstruction (PRISM3 vegetation reconstruction).

2.1.1 HadCM3

A comprehensive description of the UK Met Office Hadley Centre Coupled Model Version 3 (HadCM3) used in this study is available in Gordon et al. (2000) and Cox et al. (1999). HadCM3 has been widely used for palaeoclimate modelling, with simulations of the Last-Glacial Maximum and Mid-Holocene climates as well as the mPWP (Braconnot et al., 2007; Bragg et al., 2012; Valdes et al., 2017) and deeper time. HadCM3 is a dynamically and thermodynamically coupled atmosphere, ocean and sea ice model. The resolution of the atmosphere component is 2.5° in latitude by 3.75° in longitude, which translates to a grid spacing of 278 km by 417 km at the equator. The atmosphere model is composed of 19 layers with a time step of 30 minutes. The ocean model has a spatial resolution of 1.25° by 1.25° with 20 layers. The sea ice model contains parameterisation of ice drift and leads (Cattle et al., 1995) with a simple thermodynamic scheme.

2.1.2 MOSES Land surface scheme

A land surface scheme calculates the exchange of heat, moisture, momentum and CO_2 between the surface and atmosphere (Essery et al., 2003). The simulations included in this study use two different version of the Met Office (land) Surface Exchange Scheme (MOSES; versions 1 and 2.1) MOSES1 primarily differs from MOSES2.1 by its use of effective parameters to calculate a single surface energy balance for each grid box, while MOSES 2.1 includes a tile model (Essery et al., 2003; Best et al., 2006). In MOSES2.1, the grid boxes which were previously treated as whole are now characterised as mosaics of distinct surface types. Separate surface temperatures, shortwave and longwave radiative fluxes, sensible and latent heat fluxes, ground heat fluxes, canopy moisture contents, snow masses and snow melt rates are computed for each surface type or tile in a grid box. The different surface types recognised are broadleaf and needle leaf trees, C_3 and C_4 grasses, shrub, inland water, bare soil and ice. A grid box can be made of any combination of surface types apart from those classified as land-ice. The fractions of surface types within each grid box are modelled by TRIFFID (Falloon et al., 2011).

2.1.3 TRIFFID vegetation model

The dynamic global vegetation model (DGVM) TRIFFID computes the structure and distribution of six plant functional types (broadleaf tree, needle leaf tree, C_3 grass, C_4 grass, shrub and bare soil). The areal coverage, leaf index and canopy height of each plant type is

updated using a carbon balance approach whereby vegetation change is directed by net carbon fluxes calculated within the MOSES 2.1 land surface scheme (Cox, 2001). The carbon fluxes are derived using the coupled photosynthesis-stomatal conductance model developed by Cox et al. (1998) that utilises existing models of leaf-level photosynthesis in C_3 and C_4 plants (Collatz et al., 1991, 1992). Climate and CO_2 drive the resulting rates of photosynthesis and plant respiration. Each plant functional type (PFT) is updated over a grid box (normally every 10 model days) based on competition from other plant types, modelled using the Lotka-Volterra approach and the net carbon available. Soil carbon is increased by litter fall and is returned to the atmosphere by microbial respiration at a rate based on temperature and soil moisture (Cox 2001).

TRIFFID can be run in equilibrium and dynamic mode. The equilibrium mode is coupled asynchronously to the atmosphere model, with accumulated carbon fluxes passing through MOSES2.1 (Cox 2001). Using the equilibrium method has been shown to be successful in producing equilibrium states for the slowest variables in the model (for example, soil carbon and forest cover) by offline tests. This is often followed by a dynamic run in to allow faster varying components (such as grasses) to reach equilibrium with seasonally varying climate (Cox 2001). The modes used in this study are detailed in the methodology of this paper.

2.1.4 BIOME4

BIOME4 is a carbon and water flux model that predicts the interaction of vegetation distribution, structure and biogeochemistry (Kaplan, 2003). The model is driven by long term averages of monthly mean temperature, sunshine and precipitation and requires information on soil texture and depth to determine water holding capacity and percolation rates. There are twelve plant functional types (PFTs) whose bioclimatic limits determine whether it could be present in each grid cell. The seasonal maximum leaf area index (LAI) that maximises net primary production (NPP) for each PFT is calculated based on a daily time step simulation of soil water balance and monthly processes based calculations of canopy conductance, photosynthesis, respiration and phenological state (Kaplan, 2003; Haxeltine & Prentice, 1996). The PFT with the highest NPP is selected as the dominant plant type. For the biome to be identified, the PFTs are ranked according to a set of rules based on a number of computed biogeochemical variables, including NPP, LAI and mean annual soil moisture

(Kaplan 2003). This ranking in each grid cell controls the selection of one of twenty-seven biomes.

2.2 Boundary conditions and experimental design

In this paper, we present results from ten climate model simulations (Table 1). Four experiments were run with HadCM3 based on experimental design from the Pliocene Model Intercomparison Project (PlioMIP) (Haywood et al., 2010; Bragg et al., 2012), using PRISM3 boundary conditions (Dowsett et al., 2010) and the MOSES 1 land surface scheme with prescribed vegetation from Salzmann et al. (2008). To maintain consistency with the PlioMIP project the Pliocene experiments were set up with CO₂ concentrations at 405 ppmv. While the PlioMIP project specified a modern orbital configuration, here we have performed simulations for MIS G17, K1, KM3 and KM5c interglacials using orbital parameters derived from the Laskar et al. (2004) astronomical solution. For these interglacials the specific orbit used in the simulations represents the peak of the interglacial according to the LR04 benthic oxygen isotope stack. An additional four experiments were run with the same set up but this time in conjunction with the dynamic vegetation model TRIFFID and the MOSES 2.1 land surface scheme. All experiments were run for five hundred years with the final 100 years used to calculate the required climatological averages. Table 1 details the simulations included in this study. There were two pre-industrial experiments also run as a comparison, one with MOSES 1 land surface scheme and the other with MOSES2.1.

The experiments using TRIFFID were run using equilibrium mode (where TRIFFID is coupled to the atmospheric model, with accumulated carbon fluxes passing through MOSES 2.1 (Cox, 2001) for the first 50 years and subsequently run in dynamic mode for the remainder of the simulation (450 years). All simulations were subsequently run through BIOME4 to compare biome types between those run with prescribed vegetation and those with dynamic vegetation.

When running BIOME4 a standard anomaly method was used, which subtracts the control climate simulation from the palaeo simulation and adds the resulting 'anomaly' to the present-day baseline climatology. This approach compensates for first order bias in the HadCM3 control simulations (Kaplan, 2003). Due to the lack of sufficient observational

climatological data this method could not be employed over Antarctica, therefore biomes are only predicted up to 60°S in the Southern Hemisphere.

Haywood et al., (2013a) show that the peak of MIS KM5c is characterised by a near modern orbital forcing within a period of low eccentricity and low precession (Laskar et al., 2004; Prescott et al., 2014). In this study, therefore, when examining changes in the climatology in the simulations of the four interglacials, KM5c is considered as the control Pliocene experiment.

3. Results – Climatological response to orbital forcing

3.1 Pliocene interglacial climate differences

We have simulated four interglacials within the mPWP using prescribed (HadCM3 MOSES1) and dynamic vegetation models (HadCM3 MOSES2.1 coupled with TRIFFID). Using both versions of the model, all interglacials are warmer than the pre-industrial control experiments (range of 18.05°C to 19.45°C global annual mean temperatures). Our experiments for KM5c are similar to previous mPWP climate simulations that have modern orbit (in terms of the large-scale features of temperature and precipitation change; (Haywood et al., 2013b), due to the near modern orbital configuration during MIS KM5c (3.205 Ma). The other interglacials are between 0.54°C and 0.71°C warmer as a global annual mean average than KM5c for the prescribed vegetation experiments and between 0.51°C and 0.64°C warmer for the dynamic vegetation experiments (Table 1). Global annual mean total precipitation rate increases are between 0.04mm/day and 0.05mm/day for prescribed and 0.01mm/day and 0.03mm/day for dynamic vegetation experiments (Table 1). Experiments incorporating dynamic vegetation are on average 0.73°C warmer, as a global annual mean average, than those using prescribed, which may be attributable to either general differences in the model or the feedbacks on climate associated with the implementation of dynamic vegetation. Broadly all regional patterns of temperature and precipitation change are enhanced in the MOSES2.1 experiments relative to MOSES1 for each of the studied interglacials. The detailed climate response associated with each interglacial will be described alongside the vegetation (biome and PFT) predictions below.

3.1.1 MOSES1 prescribed vegetation experiments

The large-scale features of surface temperature change and precipitation (relative to the pre-industrial experiment) are seen in all four experiments (Figs. 2d and 2h), however the patterns of change in Plio-G17^{Prescribed}, Plio-K1^{Prescribed}, Plio-KM3^{Prescribed} are intensified (Fig. 2a-c, 2e-g). The dominant features include progressive warming towards the higher latitudes of both hemispheres, more surface warming over the land versus the oceans. There is also cooling over tropical Africa and India which is related to increases in precipitation and associated evaporative cooling and an enhanced di-pole pattern in the North Atlantic (linked to a change in the mode of sinking/deep-water formation, which has been observed previously using this version of the model (see Prescott et al., 2014)).

A key difference between experiments Plio-G17^{Prescribed}, Plio-K1^{Prescribed}, Plio-KM3^{Prescribed} and Plio-KM5c^{Prescribed} is the generally reduced seasonal range of temperature in the Southern Hemisphere versus the increased seasonal range of temperatures in the Northern Hemisphere (particularly over land). This bipolar response is understandable given the changes in orbital forcing shown in Figure 1 (b-e).

The four interglacial experiments (Plio-G17^{Prescribed}, Plio-K1^{Prescribed}, Plio-KM3^{Prescribed} and Plio-KM5c^{Prescribed}) with prescribed vegetation were run through the offline vegetation model BIOME4 to classify them into different biomes for comparison purposes (Figure 3b – e). Figure 3a shows the PRISM3 vegetation reconstruction from Salzmann et al. (2008) for reference. As the PRISM3 vegetation reconstruction is a model boundary conditions, the subsequent biome reconstructions are, in some respects, constrained to the PRISM3 dataset. Any differences are due to inconsistencies between the simulated Pliocene climate and the original vegetation reconstruction (PRISM3) or are a function of the climate response to the orbital forcing imposed.

There are regional differences in biome distribution when compared to the PRISM3 reconstruction. In all four interglacial experiments, South Africa is dominated by shrubland and desert instead of forest and woodland in the PRISM3 reconstruction. All interglacials show a larger expanse of grassland in North America and Asia, as well as enhanced desert over Australia and a loss of trees to shrubland in South America. Plio-KM5c^{Prescribed} predicts the most similar biome reconstruction to PRISM3. This is to be expected as this interglacial

has the least difference from modern orbital conditions (Haywood et al. 2013a; Prescott et al., 2014).

3.1.2 MOSES2.1 Dynamic vegetation experiments

To understand how the addition of dynamic vegetation can impact the modelled climate response to orbital forcing, as well as to further understand the changes seen in vegetation distribution, we investigate annual and seasonal surface air temperature (SAT) and precipitation changes in the four interglacials (Fig. 4) alongside the changes in the simulated vegetation (Fig. 5 and 3f-3i).

The annual SAT differences (the interglacials minus the Plio-KM5c^{Dynamic} control) show a similar pattern to the Plio-KM5c^{Dynamic} minus Pre-Ind^{Dynamic} (Fig. 4d) but with a greater magnitude of change. Interglacials Plio-G17^{Dynamic} and Plio-KM3^{Dynamic} present greater high latitude warming compared to Plio-KM5c^{Dynamic} than Plio-K1^{Dynamic}. For Plio-G17^{Dynamic} warming of ~2°C is modelled, and in Plio-KM3^{Dynamic} warming reaches 3.5°C at the high latitudes (60°N – 90°N) relative to the Plio-KM5c^{Dynamic} control experiment. Patterns of temperature change such as high latitude warming and tropical cooling are seen in all the interglacials (when differenced to Plio-KM5c^{Dynamic}) and are generally consistent with the simulations using prescribed vegetation (Fig. 2).

TRIFFID's predictions of PFTs are described to better understand the differences between the interglacials due to orbital changes and dynamic vegetation feedbacks (Fig 5). Here we discuss the results in relation to how they are different to the Plio-KM5c^{Dynamic} control broken down into different regional responses.

Africa

In Plio-KM5c^{Dynamic} there is 80-90% broadleaf forest over southern and central Africa with 100% bare soil (desert) in North Africa, Arabia and the west coast of southern Africa. The forest and bare soil are separated by a thin band of grassland at approximately 15°N.

Plio-K1^{Dynamic} and Plio-KM3^{Dynamic} show 80 – 90% increase of broadleaf trees across southern North Africa relative to the Plio-KM5c^{Dynamic} control. This replaces bare soil and the grasses

therefore pushing the boundary between forest and grassland northwards. Plio-G17^{Dynamic} shows this same pattern but broadleaf increase is over a much smaller area and is less intense. In the Plio-K1^{Dynamic} interglacial Southern Africa shows a loss of 80-100% broadleaf to bare soil and grassland, with Plio-KM3^{Dynamic} showing a slight loss of broadleaf and the occurrence of grasses.

North America

Plio-KM5c^{Dynamic} has a mixed forest of broadleaf and needle leaf trees in North America with the highest percentage of broadleaf trees predominately focussed in the northern continental interior and South East America and Mexico. The rest of America, Canada and Greenland (outside of the ice sheet) is dominated by needle leaf trees.

Plio-G17^{Dynamic}, Plio-K1^{Dynamic} and Plio-KM3^{Dynamic} share similar spatial changes in vegetation over North America. Relative to Plio-KM5c^{Dynamic}, they present 30–50% more broadleaf trees over Canada and Alaska and a reduction of the same PFT of 30-40% in Central and Eastern America. This increase of broadleaf is associated with a decrease of needle leaf trees over the same areas. There are also areas of increasing shrub (up to 60%) to the west of America replacing needle leaf trees.

South America

Within the Plio-KM5c^{Dynamic} control simulation there is forest of up to 90% broadleaf trees over most of South America. Over the remaining areas, predominantly the interior of Northern Brazil, there are areas of 85% grassland and along the east coast of Brazil, 100% bare soil. Chile and southern Argentina are dominated by needle leaf trees.

Over South America, the differences in PFTs compared to Plio-KM5c^{Dynamic} seen in interglacial peaks Plio-G17^{Dynamic}, Plio-K1^{Dynamic} and Plio-KM3^{Dynamic} are minor. However, over Brazil, Plio-G17^{Dynamic} and Plio-KM3^{Dynamic} show increases in broadleaf trees (between 20% and 60%), whereas Plio-K1^{Dynamic} shows a decrease of up to 60% over the southern East coast of Brazil.

Eurasia

Plio-KM5c^{Dynamic} shows Eurasia largely covered in forest, including 70% broadleaf forest over Spain and south-western Europe. Central Siberia and areas of southern Asia (e.g. South

China and Indonesia) have broadleaf forest concentrations reaching 95%. The remaining areas of Northern Eurasia have 50 - 75% of needle leaf trees. Grassland can be seen in India and in central Asia south of the simulated forest line. There are shrubs found in small areas throughout Asia, particularly in the north-eastern region.

All three interglacials exhibit localised increases in broadleaf trees in northern Eurasia, however, the dominant response is up to 60% decline in needle leaf trees that are replaced by grasses (20% increase) and shrubs (up to 60% increase). The largest difference in PFTs for the interglacials is in the Northern region of India where there is a 100% reduction in bare soil, replaced by grassland and broadleaf trees.

Australia

Australia in the Plio-KM5c^{Dynamic} control experiment includes large areas of broadleaf forest to the north and east of the country, grassland through the centre, surrounded by shrubland and bare soil in the south east.

Plio-G17^{Dynamic}, Plio-K1^{Dynamic} and Plio-KM3^{Dynamic} all predict a reduction in grassland in central Australia which is replaced with broadleaf forest to the north and shrub to the south. Plio-K1^{Dynamic} has a slightly more pronounced pattern of change, comprising a 60% reduction in broadleaf forest along the north-east coastline with grassland growing instead.

Antarctica

Plio-KM5c^{Dynamic} and Plio-G17^{Dynamic} predict mainly shrub and grassland over non-glaciated regions of Antarctica with small areas of bare soil. The largest changes predicted over Antarctica are within the Plio-K1^{Dynamic} interglacial. Experiment Plio-K1^{Dynamic} suggests that all grasses and shrubs on the Antarctic margins are replaced by bare soil. Experiment Plio-KM3^{Dynamic} has a similar predicted vegetation distribution with a smaller area of increased bare soil and grassland.

The addition of dynamic vegetation results is a spatially complex climatic response. There are some areas where adding vegetation causes positive feedbacks, for example, increases the temperature signal (be that, positive or negative) and examples of negative feedbacks where this signal is reduced with the addition of dynamic vegetation. There is enhanced warming over central South America (5°C anomaly in Plio-K1^{Dynamic}) and southern Africa (up

to 10°C anomaly in Plio-K1^{Dynamic}) compared to the Plio-KM5c^{Dynamic} control. This is due to feedbacks through partial replacement of forest with grasses in South America, and with grasses, shrubs and bare soil in southern Africa. The occurrence of more open type vegetation (in Africa and South America; Fig. 5) is caused by the orbitally forced warming in these areas (in Plio-K1^{Prescribed}; Fig. 2b) and enhanced by decreases in evapotranspiration (not shown). This is linked with a decrease in precipitation in the Plio-K1^{Prescribed} experiment (Fig. 2f). The larger temperature change seen in central Africa is a result of a positive feedback between vegetation and surface temperature brought about through the northward shift of the Sahara Desert and its replacement with broadleaf forest and grasses (Fig. 4 and Fig. 5).

Over India, bare soil is replaced with broadleaf forest and grasses and this change amplifies the local evapotranspiration-driven cooling demonstrated in the prescribed vegetation experiments. The largest positive feedback effect is seen in Plio-K1^{Dynamic} over Antarctica. This area shows higher albedo (not shown) due to snow cover and a temperature decrease of 3.5°C compared to Plio-KM5c^{Prescribed}. When using dynamic vegetation, the simulated albedo over Antarctica is increased further due to the total loss of vegetation (shrub and grass) and its replacement with bare soil leading to further cooling in these regions Plio-K1^{Dynamic} is up to 9°C colder than Plio-KM5c^{Dynamic}).

In the prescribed vegetation experiments we demonstrate a trend towards more open vegetation in Eurasia (Fig. 3b-e), linked primarily to changes in insolation patterns. The differences in vegetation (in terms of PFT, Fig. 5) are enhanced further by positive feedbacks in dynamic vegetation (reduction of precipitation, evapotranspiration and soil moisture associated with the loss of forest).

There are however, also areas of cooling seen in the MOSES2.1 simulations when run with dynamic vegetation that are not seen in the simulations run solely with changing orbital forcing and prescribed vegetation. For example, in all interglacial experiments, coastal northeast Brazil shows a cooling of approximate 5°C when compared to Plio-KM5c^{Dynamic} (Fig. 4a-c). This appears to be due to an orbitally driven vegetation switch from bare soil and grasses to broadleaf forest which results in an increase in evapotranspiration (and a resulting increase of the latent heat flux). Coupling the simulations to a dynamic vegetation model also induces a cooling of 2°C (in all interglacials) on the coastline of South Australia. This

temperature change occurs with the replacement of bare soil and grass with shrub, and is associated with an increase of evaporative cooling in this region (not shown).

There is a reduction in the level of high latitude warming seen with the introduction of dynamic vegetation, especially in two interglacials (Plio-KM3^{Dynamic} and Plio-G17^{Dynamic}) that show greater high latitude warming than Plio-KM5c^{Dynamic}. Broadleaf trees in the Arctic have twice the albedo and 50 – 80% greater evapotranspiration rates when leafed-out than their evergreen needle leaf counterparts (Swann et al., 2010). Therefore, more broadleaf forest replacing needle leaf along the Arctic coast has a cooling effect due to increased evapotranspiration, moderating the high northern latitude warming signal.

The cause and effect of the simulated climate response to orbit and vegetation changes is complicated when introducing the dynamic vegetation model, as this also involves a switch in land surface schemes. Where the inclusion of dynamic vegetation has made the terrestrial areas generally warmer, this could be arguably due to the use of MOSES2.1 (over MOSES1), which in previous analysis has been found to be a warmer model. However, we can suggest that the areas where the introduction of dynamic vegetation simulates an increased cooling, to be solely a signal from vegetation feedbacks.

3.2 MOSES2.1 Dynamic Large scale biome changes (BIOME4)

The four interglacial experiments (Plio-G17^{Dynamic}, Plio-K1^{Dynamic}, Plio-KM3^{Dynamic} and Plio-KM5c^{Dynamic}) with dynamic vegetation were run through the offline vegetation model BIOME4 to classify them into different biomes for comparison purposes.

Patterns of biome distribution appears similar between the four interglacials (using dynamic vegetation). They all have expanded grassland over Asia and North America, with Eastern Europe/Scandinavia predominantly showing temperate deciduous forest. They all show large areas of desert in northern and southern Africa, however three experiments (Plio-G17^{Dynamic}, Plio-K1^{Dynamic}, and Plio-KM3^{Dynamic}) show smaller desert areas with more xerophytic shrubland than Plio-KM5c^{Dynamic} over central Australia. The Arctic coastline has predominantly evergreen taiga/montane forest. South America has tropical forest biome to the north and shrubland and mixed forest types to the south.

There are detailed differences between the BIOME4 reconstructions for the dynamic vegetation experiments. For example, across central Africa Plio-K1^{Dynamic} and Plio-KM3^{Dynamic} show a band of deciduous forest, whereas Plio-G17^{Dynamic} and Plio-KM5c^{Dynamic} are more dominated by tropical savannah and shrubland biomes. In Plio-KM5c^{Dynamic}, taiga montane forest reaches the Arctic coastline and stretches latitudinally across north Asia. The other three interglacials also have taiga montane forest in this region but covering a smaller area. In experiments Plio-K1^{Dynamic} and Plio-KM3^{Dynamic} the band of forest across the coast is broken and pushed north by grassland which can reach the Arctic coast of eastern Asia. North America shows a similar pattern, with evergreen taiga/montane forest again being pushed north by grasslands which in Plio-K1^{Dynamic} and Plio-KM3^{Dynamic} reaches the northern Canadian coastline. Arid desert regions in Australia shrink in Plio-G17^{Dynamic} and Plio-KM3^{Dynamic}, whereas Plio-KM5c^{Dynamic} and Plio-K1^{Dynamic} show a distribution which is similar to the PRISM3 reconstruction of desert in this region.

In summary, the BIOME4 output for Plio-KM5c^{Dynamic} is the most like the PRISM3 reconstruction due to the stable and near modern orbital forcing. The other three interglacials run with dynamic vegetation show a very different terrestrial environment to Plio-KM5c^{Dynamic} (and the PRISM3 reconstruction). The biomes are more stratified in a latitudinal sense and are less heterogeneous with large areas of grass in the northern hemisphere mid to high latitudes.

4. Discussion

The exploration of discrete interglacial events within the mPWP was investigated in Prescott et al. (2014), which looked at both the MIS K1 and KM5c interglacial peaks and demonstrated that the two events are different in nature in terms of their climatology (Prescott et al., 2014). Here we continue with the incorporation of two more Pliocene interglacial events (MIS G17 and KM3) to build a fuller picture of mPWP interglacial climate variability, but with the addition of dynamic vegetation responses. We focus our discussion on addressing the importance of orbitally driven changes in seasonality as a driver for regional land cover response, and the validity of model predictions regarding regional palaeobotanical data.

4.1 How important is the effect of orbitally-driven seasonality changes for understanding regional climate and land cover responses, and how does the addition of a dynamic vegetation model alter the climatological and land cover response?

The simulated SATs in Figure 2 shows notably large increases in seasonal range in relation to the Plio-KM5c^{Prescribed} control simulation. For all three interglacials (G17, K1, and KM3), the larger amplitude of the Northern Hemisphere seasonal signal is forced by both the higher eccentricity (Fig. 1), when compared to MIS KM5c, and the perihelion falling during the boreal spring (MIS G17) and summer (MIS K1 and KM3).

Given the increased seasonality in all MIS G17, K1 and KM3 simulations, there is a need to understand the seasonal response of temperature in relation to predicted vegetation. For example, the cooling over Antarctica in Plio-K1^{Prescribed} is due to a large insolation reduction (of up to 100 Wm^{-2} ; Fig. 1) over the Southern Hemisphere during the summer months that is not seen to the same extent in the other interglacials. The similarities seen between all the interglacials such as northern hemisphere high latitude warming are caused by increases of up to 95 Wm^{-2} in the spring/summer months.

Changes in the seasonality of surface temperature and precipitation response is especially amplified in simulations run with dynamic vegetation (Fig. 4). In these experiments, the Northern Hemisphere shows an enhanced seasonality in all three interglacials compared to the Plio-KM5c^{Dynamic} control. While this is seen most strongly on land due to the lower heat capacity of land versus the oceans, the oceans also show the same signal. This is most clearly expressed in Plio-K1^{Dynamic} and Plio-KM3^{Dynamic} due to the largest seasonal differences in orbitally driven incoming insolation (Fig, 1).

The larger seasonal range (colder autumn/winters and warmer spring/summers) over the Northern hemisphere coincides with the reduction of forest seen in both BIOME4 output and TRIFFID PFTs in favour of more open vegetation over Eurasia. This region presented the largest vegetation change.

The colder temperatures in winter over North America/Eurasia do not reduce winter precipitation for MIS K1, G17 and KM3 compared to Plio-KM5c (in both the prescribed and

dynamic vegetation simulations). Springtime precipitation for MIS K1, G17 and KM3 increase compared to KM5c in large areas of Eurasia in experiments using prescribed vegetation. However, this is not the case for the same experiments run using dynamic vegetation where during the boreal spring and summer large areas of Eurasia receive either the same or less precipitation than the KM5c experiments, even though summer surface temperatures increase substantially. This reduced seasonal surface moisture availability can affect the seasonal patterns of warming through changes in latent heat flux, and decreased deeper soil moisture availability favouring grass/shrub occurrence over trees (Fig. 4). Grasses have an intense but shallow root system using water from upper soil layers whereas trees roots access deeper soil moisture (Ward et al., 2013). Winter precipitation is critical to recharge deeper soil layers for trees to access (Schwinning et al., 2005), and this process would be especially important in a scenario where summer temperatures increase due to a change in seasonality. Therefore, in these results the warmer spring/summers and lack of associated increase in winter/summer precipitation favours the simulation of grass rather than trees in our model simulations (Figs. 3 and 5). The reduction in available soil moisture in the deepest soil layer (on average 308 mm less in all 4 interglacials than the pre-industrial annual mean, and a decrease to 327 mm less in winter) is seen most acutely in the dynamic vegetation simulations (Suppl Fig. 8). Given that soil moisture and temperature are fundamental drivers in TRIFFID (Cox, 2001) in the prediction of vegetation types, this reduction in soil moisture provides a partial explanation for the large-scale tree retreat in Eurasia and North America.

Additionally, the higher summer temperatures seen over Eurasia and North America favours the existence of grass in the BIOME4 model. In BIOME4, through the identification of the 2 most successful PFTs each model grid cell is assigned a biome (Haxeltine & Prentice, 1996). The BIOME4 is a mechanistic model which utilises a look up table with a set value of 21°C as a maximum warm monthly mean temperature for boreal evergreen and deciduous trees to grow (Haxeltine & Prentice, 1996). The simulated mean temperature of the warmest month in our HadCM3 results often exceeds 21°C. When this threshold parameter is increased within BIOME4, the predicted forest/grass boundary moves equatorward (results not shown). It appears that this empirical threshold in BIOME4 is another explanation as to why trees are replaced with grasses in all experiments for MIS K1, KM3 and G17.

BIOME4 simulates the vegetation distribution that is in equilibrium with a particular climate and atmospheric CO₂ concentration (Haxeltine & Prentice, 1996), it does not incorporate ecological successional processes which increases the uncertainty in the results. For prediction of rapidly changing climate response, BIOME4 can suggest the general direction and maximum extent of change to be expected but this may be oversimplified. Whereas the BIOME4 model has been used offline and forced with the climatology from HadCM3 the interaction between climate and vegetation is not fully resolved. Arguably, a more realistic approach is to allow vegetation to grow and interact with the climate.

We therefore use TRIFFID, a DGVM to treat the land cover as an interactive element to ascertain the magnitude of vegetation feedbacks from orbitally forced changes in seasonality and the variability between interglacials in the mPWP. TRIFFID separates the vegetation into PFT per the physical response to climate conditions and runs interactively with the climate model, therefore enabling vegetation feedbacks that are not possible when solely running the climate through BIOME4 without TRIFFID enabled.

It is not our intention to determine which vegetation model is preferable as they adopt fundamental differences in the approach of vegetation simulation, and both have different strengths and weaknesses. In BIOME4 each grid square is assigned a biome, while this lends itself to comparison with palaeoenvironmental records, it also results in a rather binary comparison, either a match or mismatch. TRIFFID however, predicts PFTs and each grid square has the potential to contain a combination of the different PFTs allowing for a more nuanced understanding of vegetation change. There are however, only a small number of potential PFTs predicted by TRIFFID, making data-model comparison challenging but TRIFFID also has the advantage of simulating the vegetation response in a fully coupled vegetation/climate system.

When considering large scale vegetation changes predicted by TRIFFID, the decline of forest to more open vegetation (i.e. the combination of grasses, shrubs and bare soil) over Asia represents a significant change. This is consistent with the BIOME4 output which shows large expanses of grassland pushing the forest margin northwards in North America and Asia. While BIOME4 predicts temperate grassland across much of Asia, TRIFFID shows the main difference to be increased shrub causing a northward shift in broadleaf tree and an overall

reduction of needle leaf at Northern high latitudes. Given that there are such large changes of vegetation seen over Eurasia in both TRIFFID and BIOME4 we compare the general trend in these results to published palaeobotanical sites that capture variability in this region (see section 4.2).

4.2 Looking at specific high resolution records (Lake Baikal and Lake El'gygytgyn), do our simulations capture similar variability shown in the geological record?

We now consider two of the highest resolution palaeobotanical datasets currently available for the Pliocene specifically where our models simulate the clearest change due to orbital forcing (in central and eastern Asia). A similar response is also predicted over central North America but this region currently lacks a palaeobotanical record of sufficient temporal resolution to attempt to resolve the specific interglacials we have modelled. While these sites are some of the best dated terrestrial records for the Pliocene, there are still limitations in the chronologic sampling resolution. In regards to the simulations modelled here, there is not the temporal precision in the records to complete a statistically robust data-model comparison for each interglacial. Given this difficulty of precise age controls for land-based records we look to proxy time series to estimate the range of vegetation expressed during the four Pliocene interglacials at Lake El'gygytgyn in Northeast Russia and Lake Baikal in Siberia, and this range is then compared to the range in vegetation simulated by the model. Note that we appreciate that TRIFFID PFTs cannot be directly compared to abundances of pollen due to differential pollen production rates across plant types. In concert with our BIOME4 results, we instead restrict any inference regarding PFTs and reconstructed pollen types simply as a relative measure of a more open or forest covered environment. Comparison of the model output to site specific proxy data may not be statistically robust due to differences in the representation of spatial scales in the model versus the spatial regime represented by the data. In order to circumvent these limitations, we compare the vegetation reconstruction to the model grid square corresponding to the specific geographical location of the proxy data site, as well as adjacent model grid squares to better represent the overall response of the simulated vegetation in the region.

Lake El'gygytgyn

The high Arctic is particularly sensitive of late Pliocene high latitude continental climate (Andreev et al., 2016; Haywood et al., 2016a; Brigham-Grette et al., 2013). There is some suggestion from contemporary pollen studies that the lake traps pollen from a source area of several thousand square kilometres and therefore the lake provides reliable information into regional and/or even over regional vegetation changes (Lozhkin & Anderson, 2013; Andreev et al., 2016).

Detailed pollen analysis and regional climate reconstructions have been published for the late Pliocene period ~3.58 – 2.15 Ma in Andreev et al. (2014) and Brigham-Grette et al. (2013) presents a summary of multiproxy evidence from 3.58 – 2.2 Ma. Extreme warmth and polar amplification, compared to modern climate, was reconstructed from the record at Lake El'gygytgyn (67.5°, 72°) during the mPWP with a stepped cooling event during the Pliocene-Pleistocene transition (Brigham-Grette et al., 2013) and Arctic summer warmth with forest cover at both warm and cold summer orbits.

We examine pollen-based biome reconstructions of Lake El'gygytgyn (Tarasov et al., 2013) to facilitate comparison with our model results, however the fossil pollen data used for the biome reconstruction has also been the basis for other climate reconstructions (for details of this pollen analysis see Brigham-Grette et al., 2013, Melles et al., 2012 and Andreev et al., 2014).

Biome reconstructions at Lake El'gygytgyn indicate that the late Pliocene to early Pleistocene can be characterised by six vegetation types- four forest and two open vegetation biomes (Tarasov et al., 2013). The four biomes representing forest found at Lake El'gygytgyn in the Pliocene are either boreal or a mixture of boreal and temperate. The other two biomes are tundra and steppe and are dominated by boreal or arctic herb and shrub communities (Tarasov et al., 2013).

The pollen based biome reconstruction at Lake El'gygytgyn (Tarasov et al., 2013) indicates that MIS KM5c coincides with a transition from a cold deciduous biome to taiga. The pollen based biome reconstruction at KM3 is cool conifer forest (Tarasov et al., 2013) and K1 is on

the boundary between cool mixed and cold deciduous forest and tundra (Tarasov et al., 2013) whereas there is both taiga and cool conifer forest at MIS G17 (Tarasov et al., 2013).

In this modelling study, the PFTs predicted by TRIFFID for Plio-KM5c^{Dynamic} are 64% needle leaf tree, 21% shrub and 13% grass (remainder bare soil) with BIOME4 simulating a cold evergreen needle leaf forest. The surrounding grid squares show biomes varying between cold evergreen and cool evergreen needle leaf forest, and low and high shrub tundra. The main simulated biome (cold evergreen needle leaf forest), is arguably interchangeable with the taiga, predicted from the pollen data (Tarasov et al., 2013). The cold deciduous biome interpreted from the pollen data, is not represented in the simulated biomes at or around Lake El'gygytgyn in our modelling results.

The biome simulated for Plio-KM3^{Dynamic} is cold evergreen needle leaf forest at Lake El'gygytgyn, with cool conifer forest interpreted from the pollen data. The PFTs predicted by TRIFFID also show 65% needle leaf trees. For Plio-K1^{Dynamic} BIOME4 simulates cold evergreen needle leaf forest, with biomes of temperate grassland, temperate deciduous and cool mixed forest simulated in the surrounding grid squares. The pollen-based biome reconstruction shows cool mixed and cold deciduous forest moving to a tundra biome. For this interglacial the simulation of forest biome types in BIOME4 matches well with the data. TRIFFID predicts 23% shrub and 12% grass at this site which is the highest shrub percentage simulated of the interglacials.

For Plio-G17^{Dynamic} BIOME4 simulates cold evergreen needle leaf forest with cool evergreen needle leaf forest and cool mixed forest predicted in the adjacent grid squares. The pollen-based biome reconstruction shows taiga and cool conifer forest, indicating consistency with the modelling results. TRIFFID simulated PFTs also predict 67% needle leaf trees (highest of the simulated interglacials) and a drop to 19% shrub (from 23% at Plio-K1^{Dynamic}).

Lake Baikal

Lake Baikal is situated in the continental interior of north-eastern Eurasia (53°, 108°) and has a long continuous depositional history (Demske et al., 2002). Proxies suggest it was located at the boundary between different vegetation zones during the Pliocene with shifts in distribution of coniferous forests, steppe and mountain vegetation. There is an overall

cooling trend between the warm early Pliocene and the onset of Northern Hemisphere Glaciation shown by the reduction of broadleaf trees throughout the record with periods of open vegetation interpreted to have been cool, dry conditions (Demske et al., 2002).

After MIS M2 and leading up to KM5c, the proxy derived vegetation reconstruction suggests a gradual increase in spruce/hemlock forests due to an increase in precipitation. Around the KM5c event (between 3.26 and 3.18 Ma) the record indicates a decrease in forests and the spread of boreal taxa such as birches and dwarf shrubs. This corresponds to a macro fauna assemblage in West Siberia reconstructing drier and/or cooler conditions (Zykin et al., 1995).

Around KM3 there are large fluctuations in spruce abundances and pine forests begin to appear in the record leading to a reduction of spruce/hemlock forest. There is evidence of a severely dry interval five thousand years after KM3 (3.150 Ma) with low palaeotemperatures. More open vegetation spreads between KM3 and K1, with further expansion of open vegetation and dry steppe continuing to increase after K1. The pollen reconstruction at G17 shows a development of mixed coniferous forest with a specific increase in hemlock indicating a return to warmer conditions (Demske et al., 2002). There were also warm optimum conditions indicated in the record between 3.3 and 3.15 Ma and 3.01 and 2.94 Ma that envelopes all the interglacials studied here. The record in general between 3.3 and 2.9 Ma indicates variability between warm-moist conditions and cold-dry fluctuations and does not support a dry-warm climate regime.

The TRIFFID vegetation results simulate no shrub for Plio-KM5c^{Dynamic} with high percentages of broad and needle leaf trees (57% and 30% respectively). In contrast, the simulated PFTs at Plio-KM3^{Dynamic} and Plio-K1^{Dynamic} predict no broadleaf or needle leaf trees, instead predicting high shrub percentages (~60 - 70%) with the remaining vegetation simulated as grass. The simulated plant functional types show an increase of broadleaf forest (24%) at Plio-G17^{Dynamic} compared to Plio-KM3^{Dynamic} and Plio-K1^{Dynamic} with the remainder of PFTs simulated as shrub (54%) and grass (20%).

The Lake Baikal record reconstructs a varying open steppe type vegetation with mixed coniferous forest throughout the mPWP, attributing the open vegetation with MIS glacial stages. Whereas the modelled PFTs in this study simulate a mixture of predominantly forest in Plio-KM5c^{Dynamic}, no forest and mainly shrub in Plio-KM3^{Dynamic} and Plio-K1^{Dynamic} and a mix

of both forest, shrub and grass for Plio-G17^{Dynamic}. The simulated biome from BIOME4 for all four interglacials is temperate grassland at the Lake Baikal location and the surrounding area. At a glance the general trends in vegetation variability from proxy records and the PFTs simulated with TRIFFID are comparable with both indicating switches between open and forest type vegetation. The proxy based vegetation reconstruction in Demske et al. (2002) interpreted the forest vegetation to indicate warm and moist conditions and the open steppe type vegetation cold and dry. Following this, one might expect the warm interglacials modelled to simulated mainly forest vegetation at this location, however it is the two warmest of the interglacials (Plio-KM3^{Dynamic} and Plio-K1^{Dynamic}) that simulate no forest PFTs with all open vegetation types and the cooler of the two interglacials (Plio-KM5c^{Dynamic} and Plio-G17^{Dynamic}) that simulate a mixture of shrub, grass and forest PFTs. The BIOME4 results all simulate temperate grassland across this location and the surrounding areas with no variability in biomes between the interglacials.

In general, the simulated vegetation appears to be more favourable comparable to the Lake El'gygytgyn record than Lake Baikal, where in the simulated Asian continental interior a large expanse of the grassland biome is predicted by the model but not supported in the geological record. The degree to which the regional patterns of vegetation change shown in our model results truly reflect what happened during the four interglacial events in question is difficult to ascertain. Some palaeobotanical sites in the literature, especially those close to palaeogeographic transitions of major vegetation zones (Salzmann et al., 2013) present a fluctuating climate that swings between an annual climate signal of warm-wet, and cool-dry (Heusser & Morley 1996; Willis et al. 1999; Leroy & Dupont 1994; Gao et al. 2012). Whereas our model results in Eurasia for the interglacials in question show a more warm and dry signal, especially, in the northern hemisphere, where there are warmer summers of up to 14°C (relative to the control summer temperatures) as well as cooler winters (up to 5°C cooler than the control).

Palaeoclimate modelling studies by Loptson et al. (2014) and Hunter et al. (2013), both using HadCM3L coupled with TRIFFID, describe a model dry bias (associated with TRIFFID) within their results. Here, the predicted biomes also appear to reflect a dry bias but further investigation shows this loss of trees to grassland in the northern hemisphere is due to an increase of seasonality driven principally by changes in the orbital forcing. The hotter spring

and summers combined with colder autumn and winters appears to favour grass/shrub vegetation types in our simulations.

The data-model mismatch found at Lake Baikal could also be due to the proxy record not capturing the simulated interglacial peaks we have modelled here. Orbital sensitivity simulations run for the Eocene (Sloan & Morrill, 1998) also found increased seasonality in the continental temperatures which was not reflected in the proxy records. The study postulates that while this could be due to the simulations incorrectly predicting seasonal cycles, it could also be due to biases in the preservation of complete orbital cycles that prevents the stronger signals being seen in the proxy record (Sloan & Morrill, 1998). While this could also be the case for this study, the magnitude of the data-model mismatch is so substantial at Lake Baikal that it is more likely that fundamental issues with the simulations in this area and the Eurasian continental interior. The better match of data-model comparison at Lake El'gygytgyn, which is located on the Asian Arctic coastline (under a maritime influence) also suggests that the mismatch at Lake Baikal could be related to issues associated with modelling continental interiors, which has emerged in a Pliocene scenario when different to modern orbital forcing configurations have been employed.

Biases in model representations of Eurasian hydrology in response to orbital forcing have been reported before. For example, Holocene CMIP5 simulations also found drier conditions in Eurasia compared to palaeo observations that indicate this area was wetter than today (Harrison et al., 2015). For the mid-Holocene climate models simulated a significant increase in the summer temperatures in Eurasia, and therefore seasonality, whereas the observations suggest cooler summers (lower seasonality). Temperature biases in the CMIP5 modern simulations have been linked to systematic biases in evapotranspiration with an oversimplification of precipitation leading to cold temperature biases (Mueller & Seneviratne, 2014; Harrison et al., 2015). Harrison et al. (2015) suggests that some climate models do not produce a sufficient increase in regional precipitation for the mid-Holocene in Eurasia and therefore underestimate evapotranspiration causing higher summer temperatures. Interestingly, a modelling study on future climate change over Siberia using HadCM3 anomalies for a number of future scenarios, coupled to the Siberian BioClimatic model, found the climate to be drier with a reduction in forest replaced by increased steppe as a result of decreased precipitation and increasing temperatures (Tchebakova et al., 2009).

Within this study for the Pliocene we see similar trends with the simulated climate to the studies above. Increased seasonality combined with warmer summers and insufficient precipitation, and a resulting significant reduction in soil moisture, appears to create a scenario where our modelled climate is unable to sustain forest seen consistently in published records of Eurasian vegetation distribution. There is nothing in the published time series of the available records that suggest these model results are accurately simulating the vegetation of the mPWP in this region. However, due to limitations of the temporal resolution it is not possible to say for sure that the interglacials simulated are resolved in the vegetation records and the model results are therefore incorrect. Further work on generating even higher temporal resolution records from these sites would provide more conclusive comparisons.

It is important to determine whether this change in vegetation is a model specific response. While the PlioMIP project is currently in its second phase and does not include orbital sensitivity tests (Haywood et al., 2016b). The results found here add incentive for orbital sensitivity tests to be included in the third phase of the PlioMIP project, to establish whether this result is model dependant. The large changes in vegetation simulated could be in part due to the spatial resolution of the model itself. Using newer generations of models with high spatial resolution that include other earth system feedbacks, such as the interactive dust and aerosol cycles and atmospheric chemistry, may have an effect on model responses in this region (Unger & Yue, 2014; Sagoo & Storelvmo, 2017).

Another caveat in this study is the choice of CO₂ concentration for the experiments; 405 ppmv was selected to maintain consistency with the PlioMIP project. However, some high-resolution CO₂ records indicate a level of variability that has not been accounted for here. The $\delta^{11}\text{B}$ $p\text{CO}_2$ record from Martínez-Botí et al. (2015) observed orbital-scale variations of similar magnitude to that exhibited by published late and mid-Pleistocene records with the $p\text{CO}_2$ varying between 280 and 420ppm through the mid-Pliocene. Therefore, keeping the CO₂ at 405ppm in all the simulations is an oversimplification as it would have varied and potentially effected the predicted climate and vegetation response.

5. Conclusions

The mid-Pliocene Warm Period (mPWP) is an important interval to investigate the long-term response of vegetation patterns to a CO₂ induced warming. However, the nature of vegetation change in response to orbital variability during this interval is only partially constrained. Understanding orbitally induced vegetation variability is important to understand the Pliocene overall, and for identifying the degree to which climate and vegetation models are able to reproduce climate states in Earth history.

We have investigated the degree to which orbital forcing drives changes in surface climatological and land cover response between four of the largest interglacial events within the mPWP. The degree of surface temperature warming and precipitation response regionally is strongly controlled by orbital forcing. This translates into variations in seasonality and moisture availability that can have profound effects on the predictions of land cover regionally. In our study this is clearly expressed in North America and Eurasia where mid-Pliocene experiments with increased insolation during the northern hemisphere spring/summer and decreased insolation during autumn/winter (compared to a mid-Pliocene scenario with near modern orbital forcing) led to a strong climate response and associated vegetation climate feedbacks, resulting in replacement of forest with open types of vegetation. However, available high temporal resolution palaeobotanical data from Eurasia indicate that whilst variations in forest cover versus more open type vegetation are possible between interglacial events in the mPWP, trees remained a dominant feature of the landscape. This suggests that the climate and vegetation response in this region in our model is overestimated, and this conclusion is similar to studies for the mid-Holocene, using a variety of climate models, that indicate similar regional biases in climate and predicted vegetation response to orbital forcing.

This highlights the importance of evaluating model predictions using a variety of orbital scenarios and underlines the urgent requirement for additional high resolution palynological studies from around the world to better quantify the nature of land cover variability during the mPWP and the ability of climate and vegetation models to reproduce geological evidence.

Acknowledgements

All authors acknowledge receipt of funding from the European Research Council under the European Union's Seventh Framework Programme (FP7/2007-2013)/ERC grant agreement no. 278636.

References:

- Andreev, A.A., Tarasov, P.E., Wennrich, V. & Melles, M. (2016). Millennial-scale vegetation changes in the north-eastern Russian Arctic during the Pliocene/Pleistocene transition (2.7 - 2.5 Ma) inferred from the pollen record of Lake El'gygytgyn. *Quaternary Science Reviews*. [Online]. 147. p.pp. 245–258. Available from: <http://www.sciencedirect.com/science/article/pii/S0277379116301652>. [Accessed: 14 April 2017].
- Andreev, A.A., Tarasov, P.E., Wennrich, V., Raschke, E., Herzsuh, U., Nowaczyk, N.R., Brigham-Grette, J. & Melles, M. (2014). Late Pliocene and Early Pleistocene vegetation history of northeastern Russian Arctic inferred from the Lake El'gygytgyn pollen record. *Climate of the Past*. [Online]. 10 (3). p.pp. 1017–1039. Available from: <http://www.clim-past.net/10/1017/2014/cp-10-1017-2014.html>. [Accessed: 25 July 2015].
- Best, M.J., Grimmond, C.S.B. & Villani, M.G. (2006). Evaluation of the Urban Tile in MOSES using Surface Energy Balance Observations. *Boundary-Layer Meteorology*. [Online]. 118 (3). p.pp. 503–525. Available from: <http://link.springer.com/10.1007/s10546-005-9025-5>. [Accessed: 7 August 2014].
- Braconnot, P., Otto-Bliesner, B., Harrison, S., Joussaume, S., Peterchmitt, J.-Y., Abe-Ouchi, A., Crucifix, M., Driesschaert, E., Fichefet, T., Hewitt, C.D., Kageyama, M., Kitoh, A., Laîné, A., Loutre, M.-F., Marti, O., Merkel, U., Ramstein, G., Valdes, P., Weber, S.L., Yu, Y. & Zhao, Y. (2007). Results of PMIP2 coupled simulations of the Mid-Holocene and Last Glacial Maximum – Part 1: experiments and large-scale features. *Climate of the Past*. [Online]. 3 (2). p.pp. 261–277. Available from: <http://www.clim-past.net/3/261/2007/cp-3-261-2007.html>. [Accessed: 11 January 2016].
- Bragg, F.J., Lunt, D.J. & Haywood, A.M. (2012). Mid-Pliocene climate modelled using the UK Hadley Centre Model: PlioMIP Experiments 1 and 2. *Geoscientific Model Development*

- Discussions*. [Online]. 5 (2). p.pp. 837–871. Available from: <http://www.geosci-model-dev-discuss.net/5/837/2012/gmdd-5-837-2012.html>. [Accessed: 30 July 2014].
- Brigham-Grette, J., Melles, M., Minyuk, P., Andreev, A., Tarasov, P., DeConto, R., Koenig, S., Nowaczyk, N., Wennrich, V., Rosén, P., Haltia, E., Cook, T., Gebhardt, C., Meyer-Jacob, C., Snyder, J. & Herzschuh, U. (2013). Pliocene Warmth, Polar Amplification, and Stepped Pleistocene Cooling Recorded in NE Arctic Russia. *Science*. [Online]. 340 (6139). p.pp. 1421–1427. Available from: <http://www.sciencemag.org/content/340/6139/1421.abstract>. [Accessed: 14 April 2017].
- Cattle, H., Crossley, J. & Drewry, D.J. (1995). Modelling Arctic Climate Change [and Discussion]. *Philosophical Transactions of the Royal Society A: Mathematical, Physical and Engineering Sciences*. [Online]. 352 (1699). p.pp. 201–213. Available from: <http://rsta.royalsocietypublishing.org/content/352/1699/201.short>. [Accessed: 27 August 2014].
- Collatz, G., Ribas-Carbo, M. & Berry, J. (1992). Coupled Photosynthesis-Stomatal Conductance Model for Leaves of C₄ Plants. *Australian Journal of Plant Physiology*. [Online]. 19 (5). p.p. 519. Available from: http://www.publish.csiro.au/view/journals/dsp_journal_fulltext.cfm?nid=102&f=PP9920519. [Accessed: 30 July 2014].
- Collatz, G.J., Ball, J.T., Grivet, C. & Berry, J.A. (1991). Physiological and environmental regulation of stomatal conductance, photosynthesis and transpiration: a model that includes a laminar boundary layer. *Agricultural and Forest Meteorology*. [Online]. 54 (2–4). p.pp. 107–136. Available from: <http://www.sciencedirect.com/science/article/pii/0168192391900028>. [Accessed: 16 July 2014].
- Cox, P. (2001). *Description of the TRIFFID dynamic global vegetation model: Hadley Centre Technical Note 24*.
- Cox, P., Huntingford, C. & Harding, R.. (1998). A canopy conductance and photosynthesis model for use in a GCM land surface scheme. *Journal of Hydrology*. [Online]. 212–213.

p.pp. 79–94. Available from:

<http://www.sciencedirect.com/science/article/pii/S0022169498002030>. [Accessed: 28 August 2014].

Cox, P.M., Betts, R.A., Bunton, C.B., Essery, R.L.H., Rowntree, P.R. & Smith, J. (1999). The impact of new land surface physics on the GCM simulation of climate and climate sensitivity. *Climate Dynamics*. [Online]. 15 (3). p.pp. 183–203. Available from: <http://link.springer.com/10.1007/s003820050276>. [Accessed: 30 July 2014].

Demske, D., Mohr, B. & Oberhänsli, H. (2002). Late Pliocene vegetation and climate of the Lake Baikal region, southern East Siberia, reconstructed from palynological data. *Palaeogeography, Palaeoclimatology, Palaeoecology*. [Online]. 184 (1–2). p.pp. 107–129. Available from: <http://www.sciencedirect.com/science/article/pii/S0031018202002511>. [Accessed: 29 May 2015].

Dowsett, H., Barron, J. & Poore, R. (1996). Middle Pliocene sea surface temperatures: a global reconstruction. *Marine Micropaleontology*. [Online]. 27 (1–4). p.pp. 13–25. Available from: <http://www.sciencedirect.com/science/article/pii/037783989500050X>. [Accessed: 26 August 2014].

Dowsett, H., Robinson, M., Haywood, A.M., Salzmann, U., Hill, D., Sohl, L., Chandler, M., Williams, M., Foley, K. & Stoll, D. (2010). The PRISM3D paleoenvironmental reconstruction. *Stratigraphy*. [Online]. Available from: <http://nrl.northumbria.ac.uk/11399/>. [Accessed: 30 July 2014].

Dowsett, H., Thompson, R., Barron, J., Cronin, T., Fleming, F., Ishman, S., Poore, R., Willard, D. & Holtz, T. (1994). Joint investigations of the Middle Pliocene climate I: PRISM paleoenvironmental reconstructions. *Global and Planetary Change*. [Online]. 9 (3–4). p.pp. 169–195. Available from: <http://www.sciencedirect.com/science/article/pii/0921818194900159>. [Accessed: 30 July 2014].

Dowsett, H.J., Barron, J.A., Poore, R.Z., Thompson, R.S., Cronin, T.M., Ishman, S.E. & Willard, D.A. (1999). *Middle Pliocene paleoenvironmental reconstruction: PRISM 2*. [Online]. U.S.

Dept. of the Interior. Available from: <https://pubs.er.usgs.gov/publication/ofr99535>.
[Accessed: 15 September 2017].

Dowsett, H.J., Foley, K.M., Stoll, D.K., Chandler, M.A., Sohl, L.E., Bentsen, M., Otto-Bliesner, B.L., Bragg, F.J., Chan, W.-L., Contoux, C., Dolan, A.M., Haywood, A.M., Jonas, J.A., Jost, A., Kamae, Y., Lohmann, G., Lunt, D.J., Nisancioglu, K.H., Abe-Ouchi, A., Ramstein, G., Riesselman, C.R., Robinson, M.M., Rosenbloom, N.A., Salzmann, U., Stepanek, C., Strother, S.L., Ueda, H., Yan, Q. & Zhang, Z. (2013). Sea surface temperature of the mid-Piacenzian ocean: a data-model comparison. *Scientific reports*. [Online]. 3. p.p. 2013. Available from: <http://www.nature.com/articles/srep02013>. [Accessed: 5 April 2017].

Dowsett, H.J. & Poore, R.Z. (1991). Pliocene sea surface temperatures of the north atlantic ocean at 3.0 Ma. *Quaternary Science Reviews*. [Online]. 10 (2–3). p.pp. 189–204. Available from: <http://www.sciencedirect.com/science/article/pii/027737919190018P>. [Accessed: 26 August 2014].

Essery, R.L.H., Best, M.J., Betts, R.A., Cox, P.M. & Taylor, C.M. (2003). Explicit Representation of Subgrid Heterogeneity in a GCM Land Surface Scheme. *Journal of Hydrometeorology*. [Online]. 4 (3). p.pp. 530–543. Available from: [http://journals.ametsoc.org/doi/abs/10.1175/1525-7541\(2003\)004%3C0530:EROSHI%3E2.0.CO;2](http://journals.ametsoc.org/doi/abs/10.1175/1525-7541(2003)004%3C0530:EROSHI%3E2.0.CO;2). [Accessed: 28 August 2014].

Falloon, P., Betts, R., Wiltshire, A., Dankers, R., Mathison, C., McNeall, D., Bates, P. & Trigg, M. (2011). Validation of River Flows in HadGEM1 and HadCM3 with the TRIP River Flow Model. *Journal of Hydrometeorology*. [Online]. 12 (6). p.pp. 1157–1180. Available from: <http://journals.ametsoc.org/doi/full/10.1175/2011JHM1388.1>. [Accessed: 28 August 2014].

Gao, C., McAndrews, J.H., Wang, X., Menzies, J., Turton, C.L., Wood, B.D., Pei, J. & Kodors, C. (2012). Glaciation of North America in the James Bay Lowland, Canada, 3.5 Ma. *Geology*. [Online]. 40 (11). p.pp. 975–978. Available from: <http://geology.gsapubs.org/content/40/11/975.short>. [Accessed: 10 January 2016].

Gordon, C., Cooper, C., Senior, C.A., Banks, H., Gregory, J.M., Johns, T.C., Mitchell, J.F.B. & Wood, R.A. (2000). The simulation of SST, sea ice extents and ocean heat transports in a

- version of the Hadley Centre coupled model without flux adjustments. *Climate Dynamics*. [Online]. 16 (2–3). p.pp. 147–168. Available from: <http://link.springer.com/10.1007/s003820050010>. [Accessed: 30 July 2014].
- Harrison, S.P., Bartlein, P.J., Izumi, K., Li, G., Annan, J., Hargreaves, J., Braconnot, P. & Kageyama, M. (2015). Evaluation of CMIP5 palaeo-simulations to improve climate projections. *Nature Climate Change*. [Online]. 5 (8). p.pp. 735–743. Available from: <http://dx.doi.org/10.1038/nclimate2649>. [Accessed: 9 November 2015].
- Haxeltine, A. & Prentice, I.C. (1996). BIOME3: An equilibrium terrestrial biosphere model based on ecophysiological constraints, resource availability, and competition among plant functional types. *Global Biogeochemical Cycles*. [Online]. 10 (4). p.pp. 693–709. Available from: <http://doi.wiley.com/10.1029/96GB02344>. [Accessed: 21 May 2015].
- Haywood, A.M., Dolan, A.M., Pickering, S.J., Dowsett, H.J., McClymont, E.L., Prescott, C.L., Salzmann, U., Hill, D.J., Hunter, S.J., Lunt, D.J., Pope, J.O. & Valdes, P.J. (2013a). On the identification of a Pliocene time slice for data-model comparison. *Philosophical transactions. Series A, Mathematical, physical, and engineering sciences*. [Online]. 371 (2001). p.p. 20120515. Available from: <http://www.scopus.com/inward/record.url?eid=2-s2.0-84884849205&partnerID=tZOtx3y1>. [Accessed: 6 February 2017].
- Haywood, A.M., Dowsett, H.J. & Dolan, A.M. (2016a). Integrating geological archives and climate models for the mid-Pliocene warm period. *Nature Communications*. [Online]. 7 (May 2015). p.p. 10646. Available from: <http://www.nature.com/doi/10.1038/ncomms10646>. [Accessed: 5 February 2017].
- Haywood, A.M., Dowsett, H.J., Dolan, A.M., Rowley, D., Abe-Ouchi, A., Otto-Bliesner, B., Chandler, M.A., Hunter, S.J., Lunt, D.J., Pound, M. & Salzmann, U. (2016b). The Pliocene Model Intercomparison Project (PlioMIP) Phase 2: Scientific objectives and experimental design. *Climate of the Past*. [Online]. 12 (3). p.pp. 663–675. Available from: <http://www.clim-past.net/12/663/2016/>. [Accessed: 5 November 2017].
- Haywood, A.M., Dowsett, H.J., Otto-Bliesner, B., Chandler, M.A., Dolan, A.M., Hill, D.J., Lunt,

- D.J., Robinson, M.M., Rosenbloom, N., Salzmann, U. & Sohl, L.E. (2010). Pliocene Model Intercomparison Project (PlioMIP): experimental design and boundary conditions (Experiment 1). *Geoscientific Model Development*. [Online]. 3 (1). p.pp. 227–242. Available from: <http://www.geosci-model-dev.net/3/227/2010/gmd-3-227-2010.html>. [Accessed: 30 July 2014].
- Haywood, A.M., Hill, D.J., Dolan, A.M., Otto-Bliesner, B.L., Bragg, F., Chan, W.-L., Chandler, M.A., Contoux, C., Dowsett, H.J., Jost, A., Kamae, Y., Lohmann, G., Lunt, D.J., Abe-Ouchi, A., Pickering, S.J., Ramstein, G., Rosenbloom, N.A., Salzmann, U., Sohl, L., Stepanek, C., Ueda, H., Yan, Q. & Zhang, Z. (2013b). Large-scale features of Pliocene climate: results from the Pliocene Model Intercomparison Project. *Climate of the Past*. [Online]. 9 (1). p.pp. 191–209. Available from: <http://www.clim-past.net/9/191/2013/cp-9-191-2013.html>. [Accessed: 30 July 2014].
- Heusser, L.E. & Morley, J.J. (1996). Pliocene climate of Japan and environs between 4.8 and 2.8 Ma: A joint pollen and marine faunal study. *Marine Micropaleontology*. [Online]. 27 (1–4). p.pp. 85–106. Available from: <http://www.sciencedirect.com/science/article/pii/0377839895000534>. [Accessed: 21 May 2015].
- Hunter, S., Haywood, A.M., Valdes, P., Francis, J. & Pound, M. (2013). Modelling equable climates of the Late Cretaceous: Can new boundary conditions resolve data-model discrepancies? *Palaeogeography, Palaeoclimatology, Palaeoecology*. [Online]. Available from: <http://eprints.whiterose.ac.uk/80053/>. [Accessed: 11 January 2016].
- Kaplan, J.O. (2003). Climate change and Arctic ecosystems: 2. Modeling, paleodata-model comparisons, and future projections. *Journal of Geophysical Research*. [Online]. 108 (D19). p.p. 8171. Available from: <http://doi.wiley.com/10.1029/2002JD002559>. [Accessed: 15 April 2015].
- Laskar, J., Robutel, P., Joutel, F., Gastineau, M., Correia, A.C.M. & Levrard, B. (2004). A long-term numerical solution for the insolation quantities of the Earth. *Astronomy & Astrophysics*. [Online]. 428 (1). p.pp. 261–285. Available from: <https://www.aanda.org/articles/aa/pdf/2004/46/aa1335.pdf>. [Accessed: 23 May 2017].

- Leroy, S. & Dupont, L. (1994). Development of vegetation and continental aridity in northwestern Africa during the Late Pliocene: the pollen record of ODP site 658. *Palaeogeography, Palaeoclimatology, Palaeoecology*. [Online]. 109 (2–4). p.pp. 295–316. Available from: <http://www.sciencedirect.com/science/article/pii/0031018294901813>. [Accessed: 21 May 2015].
- Lisiecki, L.E. & Raymo, M.E. (2005). A Pliocene-Pleistocene stack of 57 globally distributed benthic $\delta^{18}\text{O}$ records. *Paleoceanography*. [Online]. 20 (1). p.p. n/a-n/a. Available from: <http://doi.wiley.com/10.1029/2004PA001071>. [Accessed: 10 July 2014].
- Loptson, C.A., Lunt, D.J. & Francis, J.E. (2014). Investigating vegetation–climate feedbacks during the early Eocene. *Climate of the Past*. [Online]. 10 (2). p.pp. 419–436. Available from: <http://www.clim-past.net/10/419/2014/cp-10-419-2014.html>. [Accessed: 11 January 2016].
- Lozhkin, A. V. & Anderson, P.M. (2013). Vegetation responses to interglacial warming in the Arctic: Examples from Lake El'gygytgyn, Far East Russian Arctic. *Climate of the Past*. [Online]. 9 (3). p.pp. 1211–1219. Available from: www.clim-past.net/9/1211/2013/. [Accessed: 14 April 2017].
- Lunt, D.J., Haywood, A.M., Schmidt, G.A., Salzmann, U., Valdes, P.J., Dowsett, H.J. & Loptson, C.A. (2012). On the causes of mid-Pliocene warmth and polar amplification. *Earth and Planetary Science Letters*. [Online]. 321–322. p.pp. 128–138. Available from: <http://www.sciencedirect.com/science/article/pii/S0012821X12000027>. [Accessed: 28 May 2015].
- Martínez-Botí, M.A., Foster, G.L., Chalk, T.B., Rohling, E.J., Sexton, P.F., Lunt, D.J., Pancost, R.D., Badger, M.P.S. & Schmidt, D.N. (2015). Plio-Pleistocene climate sensitivity evaluated using high-resolution CO₂ records. *Nature*. [Online]. 518 (7537). p.pp. 49–54. Available from: <https://www.nature.com/nature/journal/v518/n7537/pdf/nature14145.pdf>. [Accessed: 29 August 2017].
- Melles, M., Brigham-Grette, J., Minyuk, P.S., Nowaczyk, N.R., Wennrich, V., DeConto, R.M.,

- Anderson, P.M., Andreev, A.A., Coletti, A., Cook, T.L., Haltia-Hovi, E., Kukkonen, M., Lozhkin, A. V., Rosén, P., Tarasov, P., Vogel, H. & Wagner, B. (2012). 2.8 Million Years of Arctic Climate Change from Lake El'gygytgyn, NE Russia. *Science*. [Online]. 337 (6092). Available from: <http://science.sciencemag.org/content/337/6092/315>. [Accessed: 14 April 2017].
- Mueller, B. & Seneviratne, S.I. (2014). Systematic land climate and evapotranspiration biases in CMIP5 simulations. *Geophysical research letters*. [Online]. 41 (1). p.pp. 128–134. Available from: <http://www.pubmedcentral.nih.gov/articlerender.fcgi?artid=4459216&tool=pmcentrez&rendertype=abstract>. [Accessed: 5 March 2016].
- Pagani, M., Liu, Z., LaRiviere, J. & Ravelo, A.C. (2010). High Earth-system climate sensitivity determined from Pliocene carbon dioxide concentrations. *Nature Geoscience*. [Online]. 3 (1). p.pp. 27–30. Available from: <http://www.nature.com/doi/10.1038/ngeo724>. [Accessed: 18 June 2017].
- Prescott, C.L., Haywood, A.M., Dolan, A.M., Hunter, S.J., Pope, J.O. & Pickering, S.J. (2014). Assessing orbitally-forced interglacial climate variability during the mid-Pliocene Warm Period. *Earth and Planetary Science Letters*. [Online]. 400. p.pp. 261–271. Available from: <http://www.sciencedirect.com/science/article/pii/S0012821X1400332X>. [Accessed: 14 July 2014].
- Raymo, M.E., Hearty, P., De Conto, R., O'Leary, M., Dowsett, H.J., Robinson, M.H. & Mitrovica, J.X. (2009). PLIOMAX: Pliocene maximum sea level project. *PAGES News*. [Online]. 17 (2). p.pp. 58–59. Available from: http://moraymo.us/wp-content/uploads/2014/04/2009_raymoetal.pdf. [Accessed: 25 September 2017].
- Sagoo, N. & Storelvmo, T. (2017). Testing the sensitivity of past climates to the indirect effects of dust. *Geophysical Research Letters*. [Online]. 44 (11). p.pp. 5807–5817. Available from: <http://doi.wiley.com/10.1002/2017GL072584>. [Accessed: 18 June 2017].
- Salzmann, U., Dolan, A.M., Haywood, A.M., Chan, W.-L., Voss, J., Hill, D.J., Abe-Ouchi, A., Otto-Bliesner, B., Bragg, F.J., Chandler, M.A., Contoux, C., Dowsett, H.J., Jost, A., Kamae,

- Y., Lohmann, G., Lunt, D.J., Pickering, S.J., Pound, M.J., Ramstein, G., Rosenbloom, N.A., Sohl, L., Stepanek, C., Ueda, H. & Zhang, Z. (2013). Challenges in quantifying Pliocene terrestrial warming revealed by data–model discord. *Nature Climate Change*. [Online]. 3 (11). p.pp. 969–974. Available from: <http://dx.doi.org/10.1038/nclimate2008>. [Accessed: 15 August 2014].
- Salzmann, U., Haywood, A.M., Lunt, D.J., Valdes, P.J. & Hill, D.J. (2008). A new global biome reconstruction and data-model comparison for the Middle Pliocene. *Global Ecology and Biogeography*. [Online]. 17 (3). p.pp. 432–447. Available from: <http://doi.wiley.com/10.1111/j.1466-8238.2008.00381.x>. [Accessed: 18 June 2017].
- Schwinnig, S., Starr, B.I. & Ehleringer, J.R. (2005). Summer and winter drought in a cold desert ecosystem (Colorado Plateau) part I: effects on soil water and plant water uptake. *Journal of Arid Environments*. [Online]. 60 (4). p.pp. 547–566. Available from: <http://www.sciencedirect.com/science/article/pii/S0140196304001417>. [Accessed: 11 April 2017].
- Seki, O., Foster, G.L., Schmidt, D.N., Mackensen, A., Kawamura, K. & Pancost, R.D. (2010). Alkenone and boron-based Pliocene pCO₂ records. *Earth and Planetary Science Letters*. [Online]. 292 (1–2). p.pp. 201–211. Available from: <http://www.sciencedirect.com/science/article/pii/S0012821X10000816>. [Accessed: 5 April 2017].
- Sloan, L.C. & Morrill, C. (1998). Orbital forcing and Eocene continental temperatures. *Palaeogeography, Palaeoclimatology, Palaeoecology*. [Online]. 144 (1–2). p.pp. 21–35. Available from: <http://www.sciencedirect.com/science/article/pii/S0031018298000911>. [Accessed: 16 March 2016].
- Swann, A.L., Fung, I.Y., Levis, S., Bonan, G.B. & Doney, S.C. (2010). Changes in Arctic vegetation amplify high-latitude warming through the greenhouse effect. *Proceedings of the National Academy of Sciences of the United States of America*. [Online]. 107 (4). p.pp. 1295–300. Available from: <http://www.pnas.org/content/107/4/1295.short>. [Accessed: 16 July 2014].
- Tarasov, P.E., Andreev, A.A., Anderson, P.M., Lozhkin, A. V., Leipe, C., Haltia, E., Nowaczyk,

- N.R., Wennrich, V., Brigham-Grette, J. & Melles, M. (2013). A pollen-based biome reconstruction over the last 3.562 million years in the Far East Russian Arctic – new insights into climate–vegetation relationships at the regional scale. *Climate of the Past*. [Online]. 9 (6). p.pp. 2759–2775. Available from: <http://www.clim-past.net/9/2759/2013/cp-9-2759-2013.html>. [Accessed: 25 July 2015].
- Tchebakova, N.M., Parfenova, E. & Soja, A.J. (2009). The effects of climate, permafrost and fire on vegetation change in Siberia in a changing climate. *Environmental Research Letters*. [Online]. 4 (4). p.p. 45013. Available from: <http://iopscience.iop.org/article/10.1088/1748-9326/4/4/045013>. [Accessed: 16 March 2016].
- Thompson, R.S. & Fleming, R.F. (1996). Middle Pliocene vegetation: reconstructions, paleoclimatic inferences, and boundary conditions for climate modeling. *Marine Micropaleontology*. [Online]. 27 (1–4). p.pp. 27–49. Available from: <http://www.sciencedirect.com/science/article/pii/0377839895000518>. [Accessed: 29 July 2014].
- Unger, N. & Yue, X. (2014). Strong chemistry-climate feedbacks in the Pliocene. *Geophysical Research Letters*. [Online]. 41 (2). p.pp. 527–533. Available from: <http://doi.wiley.com/10.1002/2013GL058773>. [Accessed: 18 June 2017].
- Valdes, P.J., Armstrong, E., Badger, M.P.S., Bradshaw, C.D., Bragg, F., Davies-Barnard, T., Day, J.J., Farnsworth, A., Hopcroft, P.O., Kennedy, A.T., Lord, N.S., Lunt, D.J., Marzocchi, A., Parry, L.M., Roberts, W.H.G., Stone, E.J., Tourte, G.J.L. & Williams, J.H.T. (2017). The BRIDGE HadCM3 family of climate models: HadCM3@Bristol v1.0. *Geoscientific Model Development Discussions*. [Online]. p.pp. 1–42. Available from: <http://www.geosci-model-dev-discuss.net/gmd-2017-16/>. [Accessed: 25 April 2017].
- Ward, D., Wiegand, K. & Getzin, S. (2013). Walter’s two-layer hypothesis revisited: back to the roots! *Oecologia*. [Online]. 172 (3). p.pp. 617–30. Available from: <http://www.pubmedcentral.nih.gov/articlerender.fcgi?artid=3679411&tool=pmcentrez&rendertype=abstract>. [Accessed: 5 April 2016].
- Willis, K.J., Kleczkowski, A. & Crowhurst, S.J. (1999). 124,000-year periodicity in terrestrial

vegetation change during the late Pliocene epoch. *Nature*. [Online]. 397 (6721). p.pp. 685–688. Available from: <http://dx.doi.org/10.1038/17783>. [Accessed: 25 July 2015].

Wu, F., Fang, X., Herrmann, M., Mosbrugger, V. & Miao, Y. (2011). Extended drought in the interior of Central Asia since the Pliocene reconstructed from sporopollen records. *Global and Planetary Change*. [Online]. 76 (1–2). p.pp. 16–21. Available from: <http://adsabs.harvard.edu/abs/2011GPC....76...16W>. [Accessed: 25 July 2015].

Zykin, V.S., Zazhigin, V.S. & Zykina, V.S. (1995). Changes in environment and climate during early Pliocene in the southern West-Siberian Plain. *Russ. Geol. Geophys.* [Online]. 36. p.pp. 37–47. Available from: https://scholar.google.co.uk/scholar?q=Environmental+climate+changes+West+Siberian+Plain+pliocene+zykin+1995&btnG=&hl=en&as_sdt=0%2C5#0. [Accessed: 11 January 2016].

ACCEPTED MANUSCRIPT

Figures:

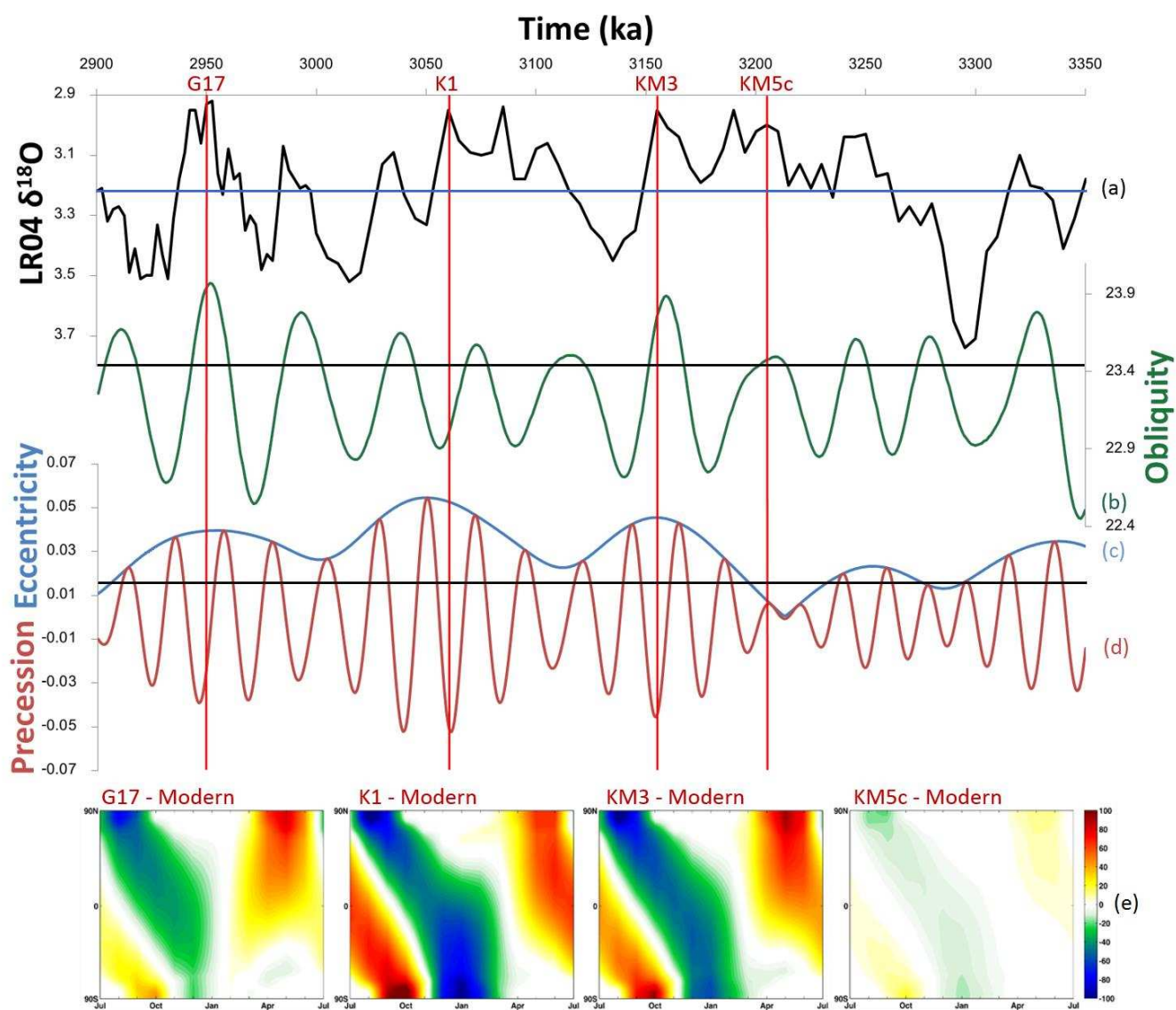


Figure 1. Marine isotope stages G17, K1, KM3 and KM5c plotted on (a) the benthic isotope record of Lisiecki and Raymo (2005). (b) Obliquity, (c) eccentricity, (d) precession as derived from the astronomical solution of Laskar et al. (2004). Black horizontal lines show modern orbit with blue horizontal line showing the Holocene oxygen isotope average. (e) Incoming short wave radiation flux derived from HadCM3 (Wm^{-2}) for MIS G17 minus modern; MIS K1 minus modern, MIS KM3 minus modern; MIS KM5c minus modern.

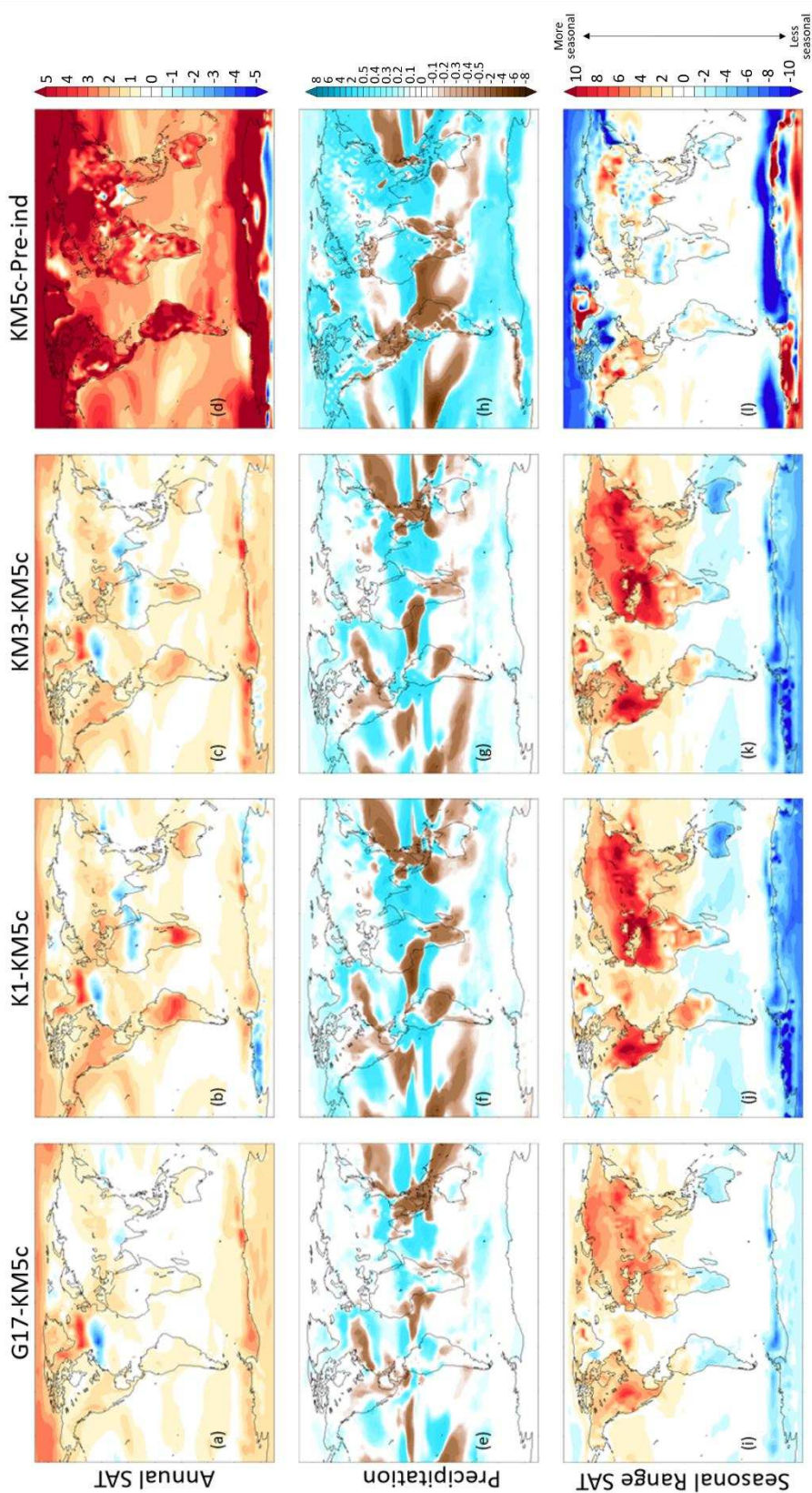


Figure 2. HadCM3 results run with MOSES1 surface scheme showing (a – d) Annual SAT anomalies ($^{\circ}\text{C}$) for (a) $\text{Plio-G17}^{\text{Prescribed}} - \text{Plio-KM5c}^{\text{Prescribed}}$, (b) $\text{Plio-K1}^{\text{Prescribed}} - \text{Plio-KM5c}^{\text{Prescribed}}$, (c) $\text{Plio-KM3}^{\text{Prescribed}} - \text{Plio-KM5c}^{\text{Prescribed}}$, (d) $\text{Plio-KM5c}^{\text{Prescribed}} - \text{Pre-Ind}^{\text{Prescribed}}$. (e – h) Annual precipitation anomalies

(mm/day) for (e) $G17^{\text{Prescribed}} - \text{Plio-KM5c}^{\text{Prescribed}}$, (f) $\text{Plio-K1}^{\text{Prescribed}} - \text{Plio-KM5c}^{\text{Prescribed}}$, (g) $\text{Plio-KM3}^{\text{Prescribed}} - \text{Plio-KM5c}^{\text{Prescribed}}$, (h) $\text{Plio-KM5c}^{\text{Prescribed}} - \text{Pre-Ind}^{\text{Prescribed}}$. (i – l) Seasonal range surface temperature anomalies ($^{\circ}\text{C}$); each figure shows the difference between the experiment and the control for the mean of the warmest month minus the mean of the coldest month. (i) $\text{Plio-G17}^{\text{Prescribed}} - \text{Plio-KM5c}^{\text{Prescribed}}$, (j) $\text{Plio-K1}^{\text{Prescribed}} - \text{Plio-KM5c}^{\text{Prescribed}}$, (k) $\text{Plio-KM3}^{\text{Prescribed}} - \text{Plio-KM5c}^{\text{Prescribed}}$, (l) $\text{Plio-KM5c}^{\text{Prescribed}} - \text{Pre-Ind}^{\text{Prescribed}}$.

ACCEPTED MANUSCRIPT

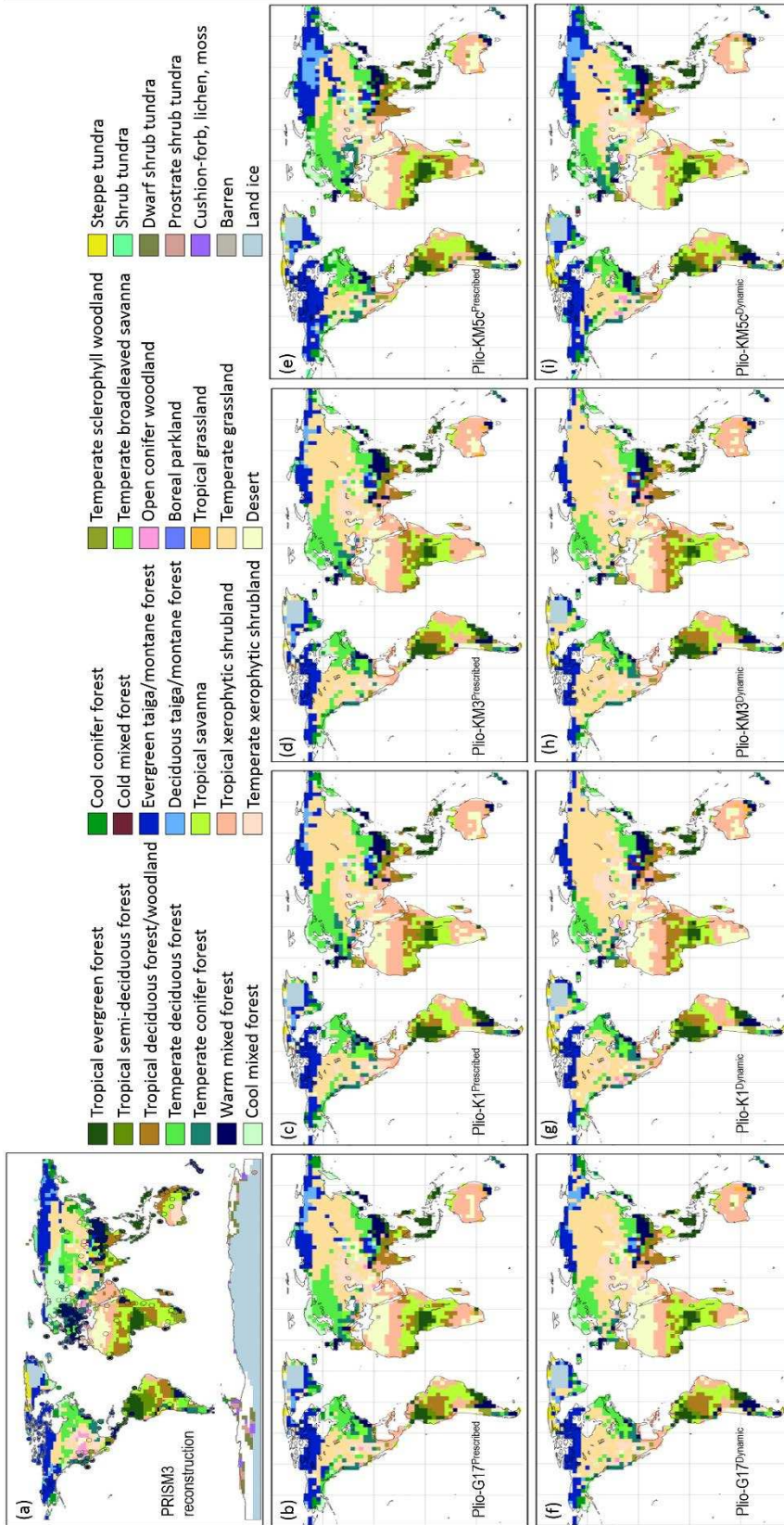


Figure 3. (a) PRISM3 vegetation reconstruction from Salzmann et al. (2008), a data/model hybrid. (b – E) Global Pliocene predicted biomes simulated by BIOME4 with experiments run with prescribed vegetation with HadCM3 and land surface scheme MOSES1. (f – i) Global Pliocene predicted biomes simulated by BIOME4 with experiments run with HadCM3 coupled to TRIFFID vegetation model and Land surface scheme MOSES2. Note the larger expanse of grassland throughout Asia, especially with experiments where vegetation was allowed to run dynamically (f – i).

ACCEPTED MANUSCRIPT

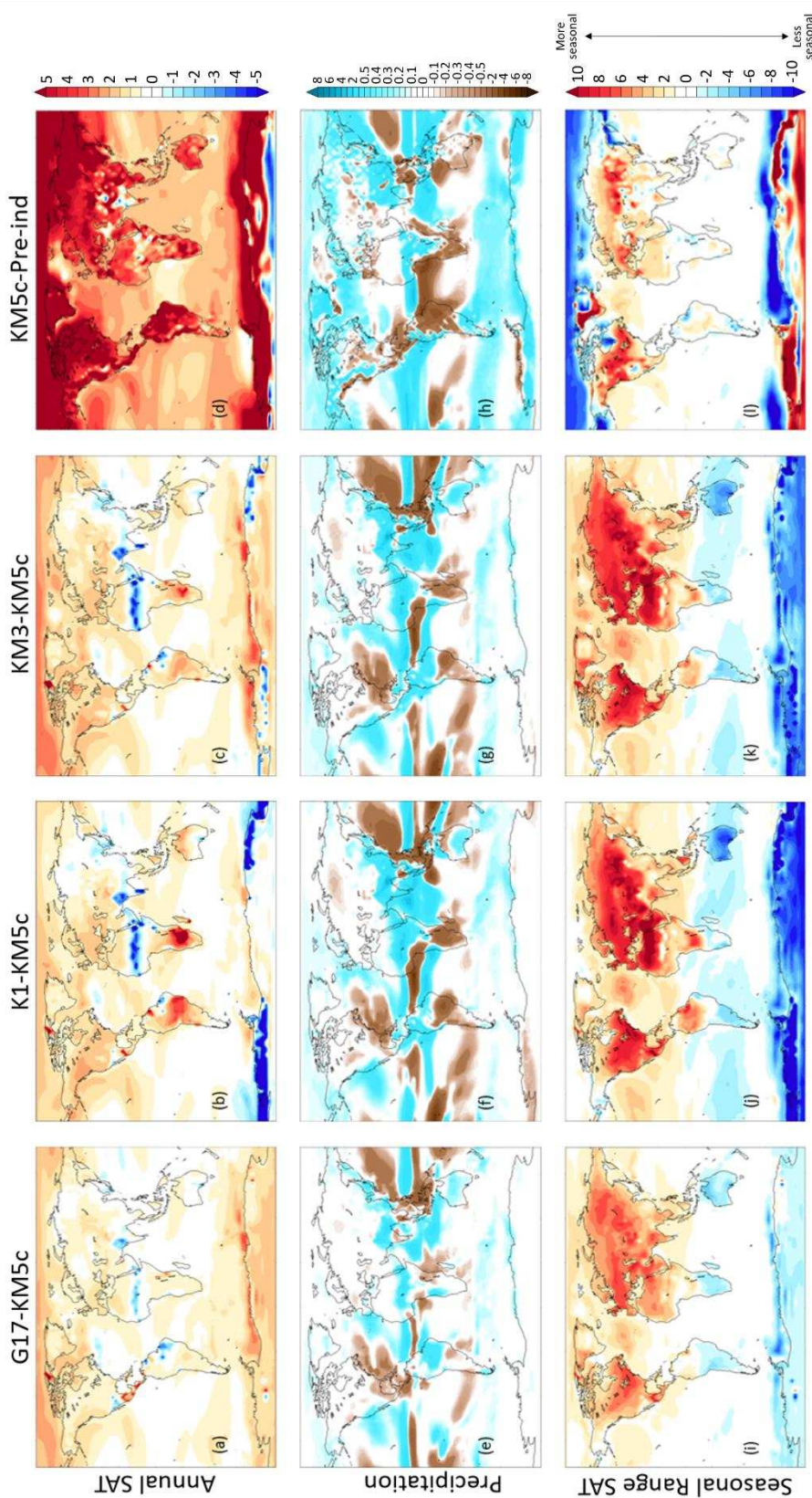


Figure 4. HadCM3 results run with MOSES2 surface scheme showing (a – d) Annual SAT anomalies ($^{\circ}\text{C}$) for (a) $\text{Plio-G17}^{\text{Dynamic}} - \text{Plio-KM5c}^{\text{Dynamic}}$, (b) $\text{Plio-K1}^{\text{Dynamic}} - \text{Plio-KM5c}^{\text{Dynamic}}$, (c) $\text{Plio-KM3}^{\text{Dynamic}} - \text{Plio-KM5c}^{\text{Dynamic}}$, (d) $\text{Plio-KM5c}^{\text{Dynamic}} - \text{Pre-Ind}^{\text{Dynamic}}$. (e – h) Annual precipitation anomalies (mm/day) for (e)

G17^{Dynamic} – Plio-KM5c^{Dynamic}, (f) Plio-K1^{Dynamic} – Plio-KM5c^{Dynamic}, (g) Plio-KM3^{Dynamic} – Plio-KM5c^{Dynamic}, (h) Plio-KM5c^{Dynamic} – Pre-Ind^{Dynamic}. (i – l) Seasonal range surface temperature anomalies (°C); each figure shows the difference between the experiment and the control for the mean of the warmest month minus the mean of the coldest month. (i) Plio-G17^{Dynamic} – Plio-KM5c^{Dynamic}, (j) Plio-K1^{Dynamic} – Plio-KM5c^{Dynamic}, (k) Plio-KM3^{Dynamic} – Plio-KM5c^{Dynamic}, (l) Plio-KM5c^{Dynamic} – Pre-Ind^{Dynamic}.

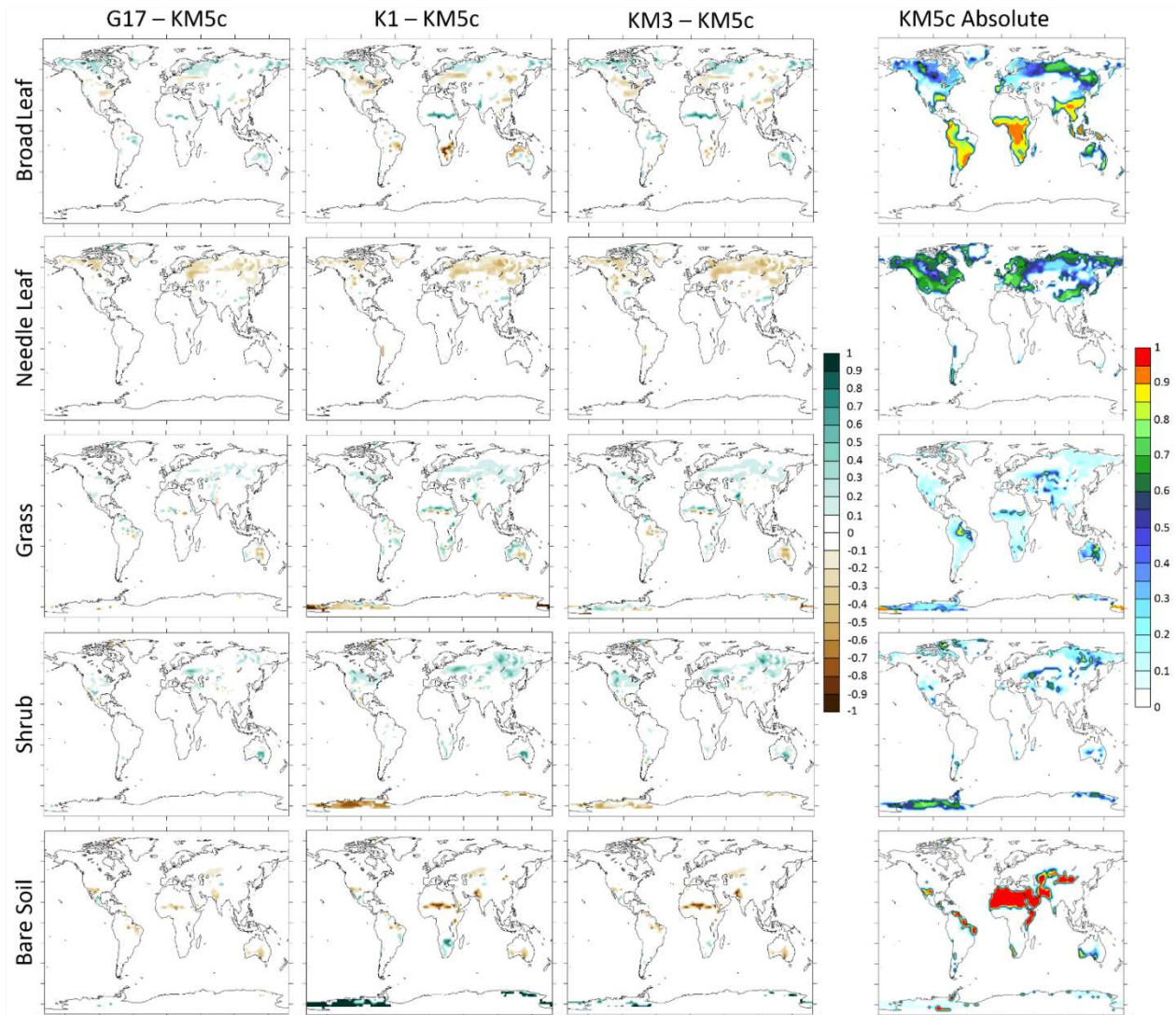


Figure 5. Model predictions experiments run with dynamic vegetation for TRIFFID predicted Plant Functional Types (PFTs) shown as percentage anomalies from control run MIS KM5c (Plio-KM5c^{Dynamic}) for (left) Plio-G17^{Dynamic} – Plio-KM5c^{Dynamic}; (middle-left) Plio-K1^{Dynamic} – Plio-KM5c^{Dynamic}; (middle-right) Plio-KM3^{Dynamic} – Plio-KM5c^{Dynamic}; (right) Control Plio-KM5c^{Dynamic} absolute plant functional types.

| Experiment name | Land Surface Scheme | Vegetation | Orbit (kyr) | Eccentricity | Precession | Obliquity (degrees) | MAT °C | MAP mm/day | JJA °C | DJF °C | JJA mm/day | DJF mm/day |
|---------------------------------------|---------------------|------------|----------------|--------------|------------|---------------------|--------|------------|--------|--------|------------|------------|
| Plio-G17 ^{Dynamic} | MOSES 2.1 | Dynamic | 2950 | 0.04 | -0.01776 | 23.96 | 19.35 | 3.04 | 22.45 | 16.35 | 3.10 | 2.99 |
| Plio-K1 ^{Dynamic} | MOSES 2.1 | Dynamic | 3060 | 0.05 | -0.05086 | 23.01 | 19.35 | 3.04 | 22.95 | 16.05 | 2.95 | 3.11 |
| Plio-KM3 ^{Dynamic} | MOSES 2.1 | Dynamic | 3155 | 0.05 | -0.04350 | 23.76 | 19.45 | 3.02 | 23.15 | 16.15 | 3.01 | 3.02 |
| Plio-KM5c^{Dynamic} | MOSES 2.1 | Dynamic | 3205 | 0.01 | 0.00605 | 23.47 | 18.85 | 3.01 | 21.25 | 16.55 | 3.06 | 2.98 |
| Pre-Ind^{Dynamic} | MOSES 2.1 | Dynamic | Pre-Industrial | 0.02 | 0.01628 | 23.44 | 14.85 | 2.91 | 17.15 | 13.05 | 2.98 | 2.87 |
| Plio-G17 ^{Prescribed} | MOSES 1 | Prescribed | 2950 | 0.04 | -0.01776 | 23.96 | 18.55 | 3.10 | 21.25 | 15.85 | 3.18 | 3.02 |
| Plio-K1 ^{Prescribed} | MOSES 1 | Prescribed | 3060 | 0.05 | -0.05086 | 23.01 | 18.75 | 3.10 | 21.85 | 15.85 | 3.07 | 3.11 |
| Plio-KM3 ^{Prescribed} | MOSES 1 | Prescribed | 3155 | 0.05 | -0.04350 | 23.76 | 18.75 | 3.11 | 21.85 | 15.75 | 3.13 | 3.07 |
| Plio-KM5c^{Prescribed} | MOSES 1 | Prescribed | 3205 | 0.01 | 0.00605 | 23.47 | 18.05 | 3.06 | 20.05 | 15.95 | 3.14 | 3.00 |
| Pre-Ind^{Prescribed} | MOSES 1 | Prescribed | Pre-Industrial | 0.02 | 0.01628 | 23.44 | 13.85 | 2.88 | 15.65 | 11.95 | 2.96 | 2.83 |

Table 1. Summary of experiments including orbital parameters implemented in HadCM3, also showing global mean annual and seasonal temperatures and precipitation. Control experiments indicated in bold.

Highlights:

- Four interglacial events in the mid-Piacenzian have been modelled using HadCM3.
- With different orbital forcing which controls regional surface climate responses.
- There is resulting variations in seasonality and moisture availability.
- Replacement of forest with open types of vegetation in simulated in Eurasia.
- This change in vegetation is not seen in available palaeobotanical data in this area.

ACCEPTED MANUSCRIPT

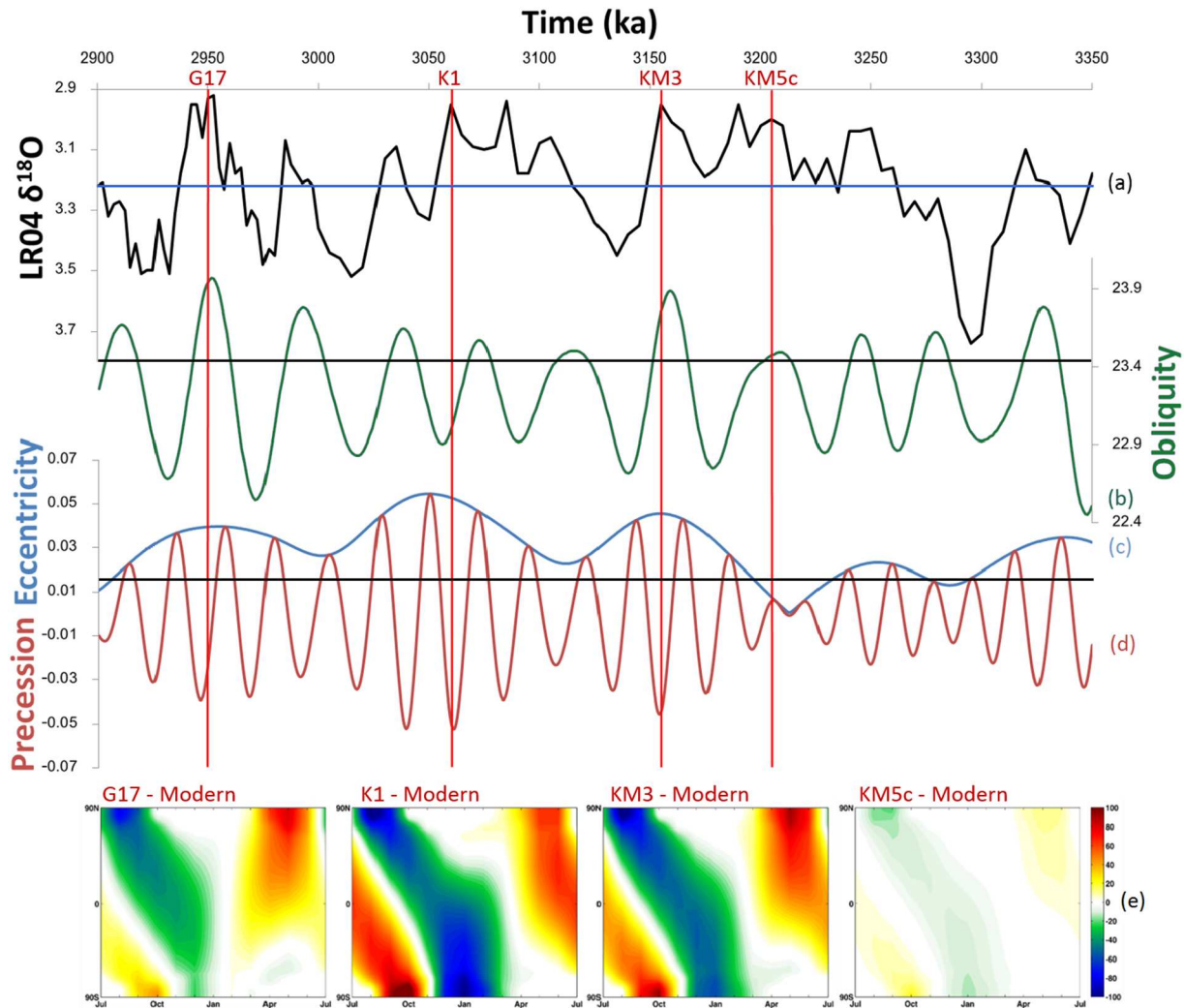


Figure 1

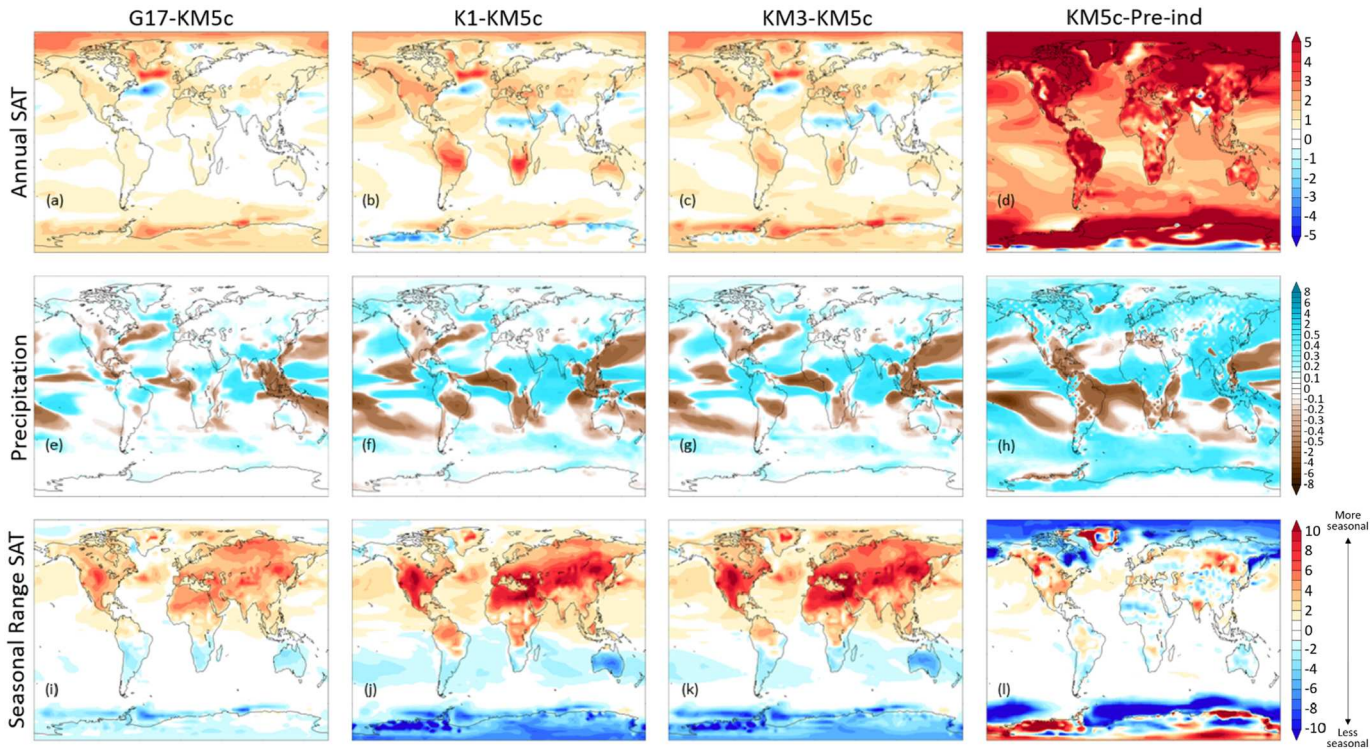


Figure 2

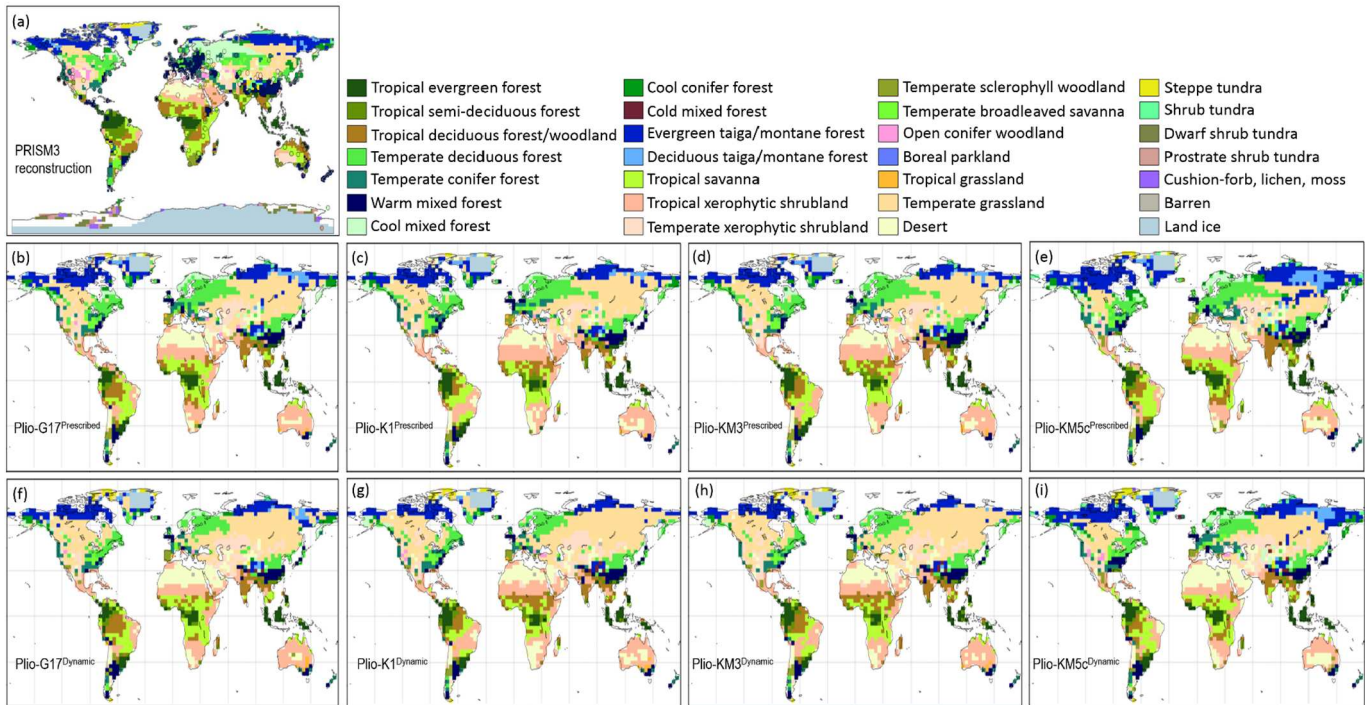


Figure 3

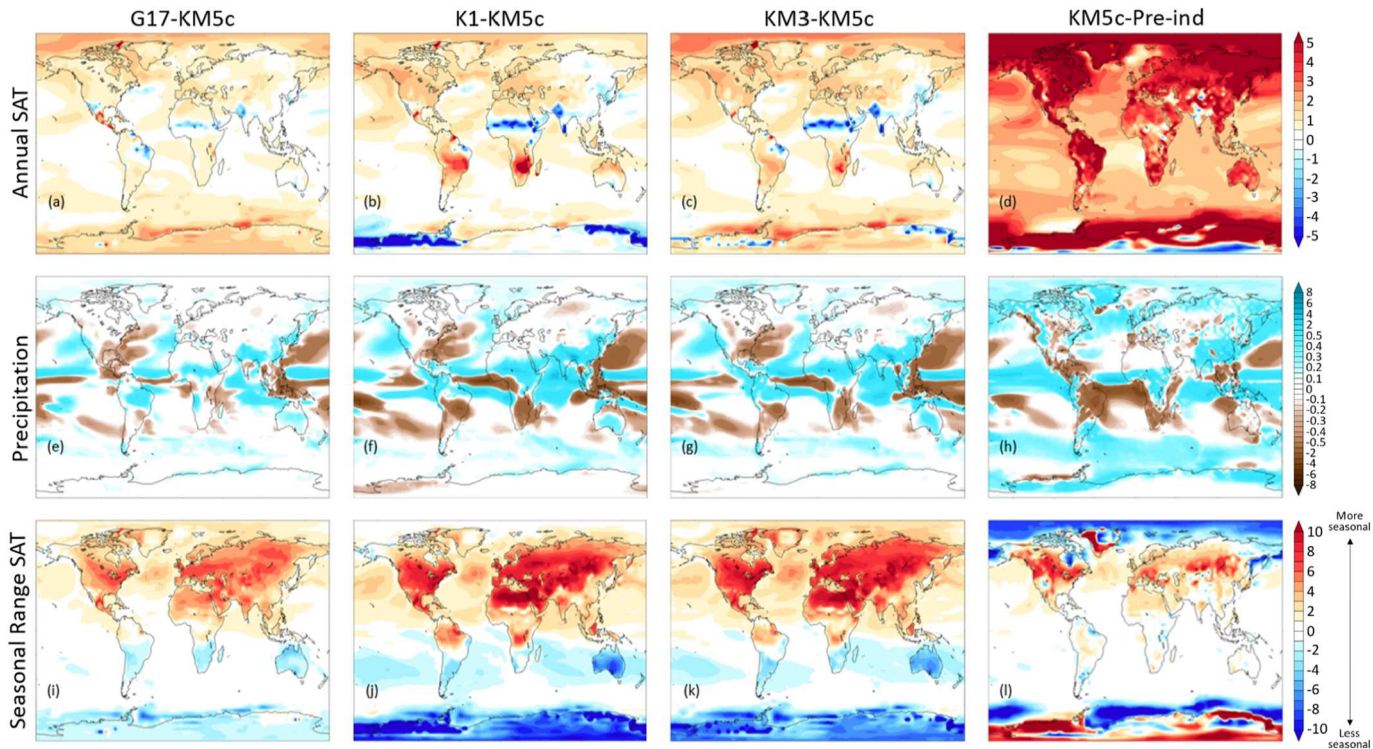


Figure 4

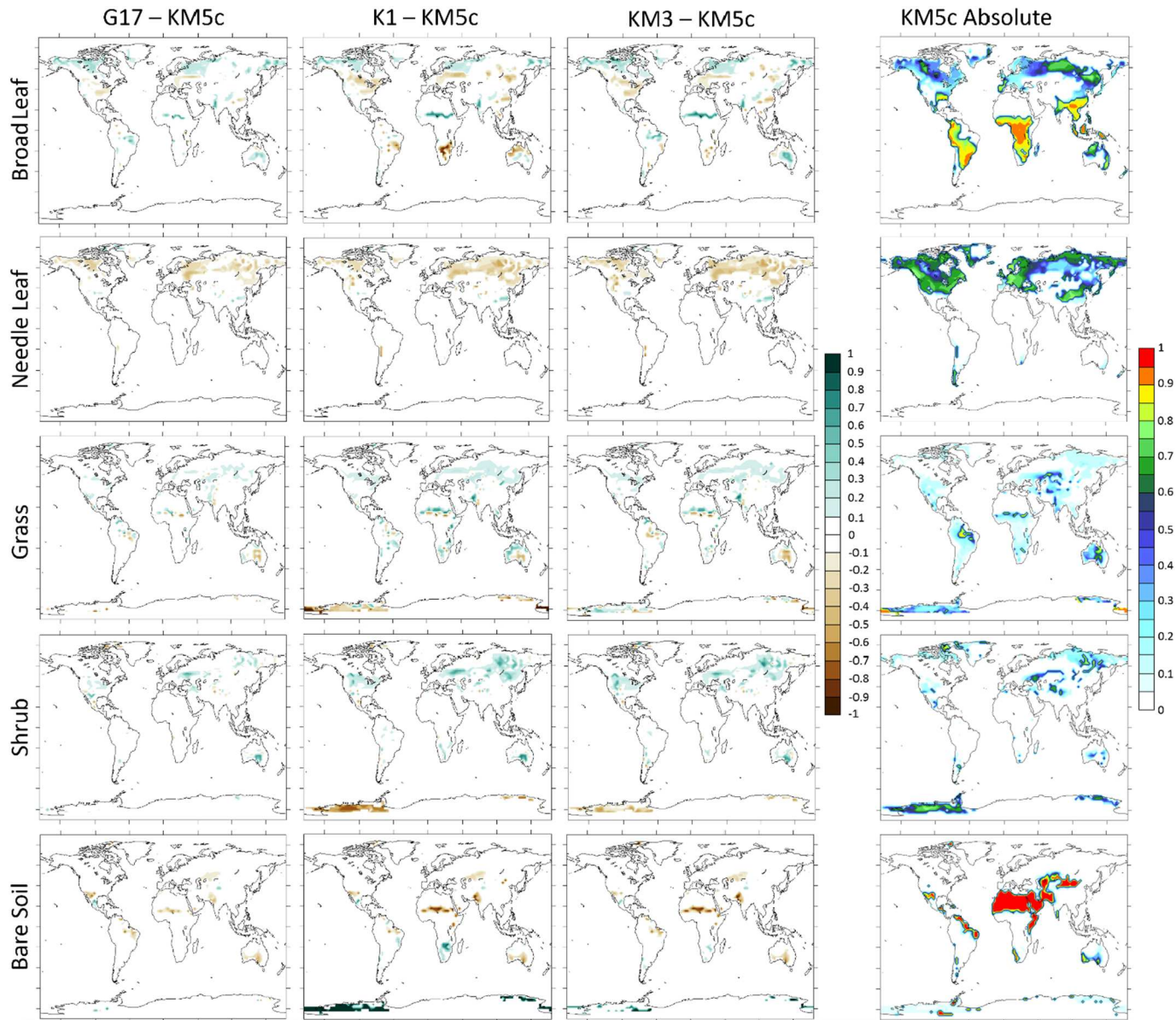


Figure 5